Restriction of reaction sites on metal-sulfide cores induced by steric repulsion of bis-N-heterocyclic carbene ligands in trinuclear complexes bearing triply bridging sulfide ligands.

Natsuki Yabune, Hiroshi Nakajima and Takanori Nishioka*

Division of Molecular Materials Science, Graduate School of Science, Osaka City University, Osaka 558-8585, Japan.

Department of Chemistry, Graduate School of Science, Osaka Metropolitan University, Osaka 558-8585, Japan. E-mail: nishioka@omu.ac.jp.

Supplementary Information

1. ^{1}H NMR spectra of the complexes at 253 K and at 293 K

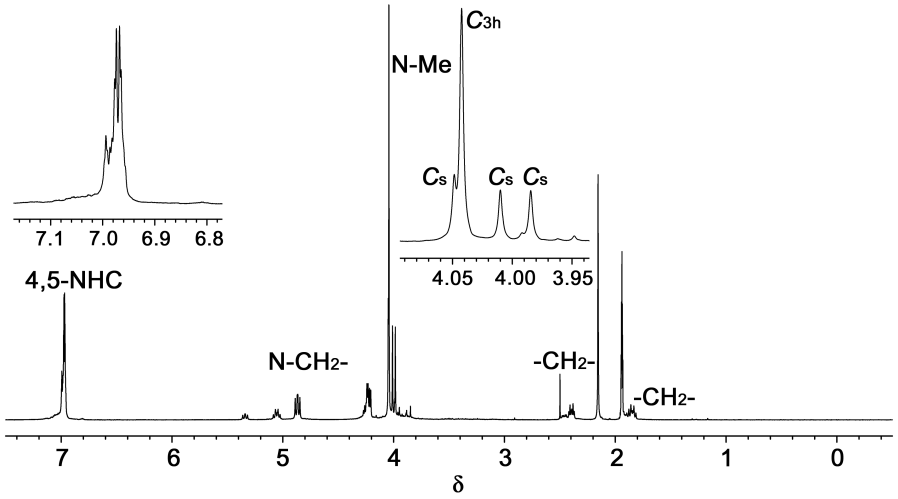

Fig. S1 ^{1}H NMR spectrum of triplatinum complex with bisNHC-C3 ligands, $[\mathbf{Pt}^{\mathbf{C3}}_{\mathbf{3}}]^{2+}$, at 293 K (600 MHz, CD_3CN). Three and one sets of signals attributed to bisNHC ligands of the unsymmetric C_s- and symmetric C_{3h}-isomers were observed, especially the signals in the N-Me region were clearly separated.

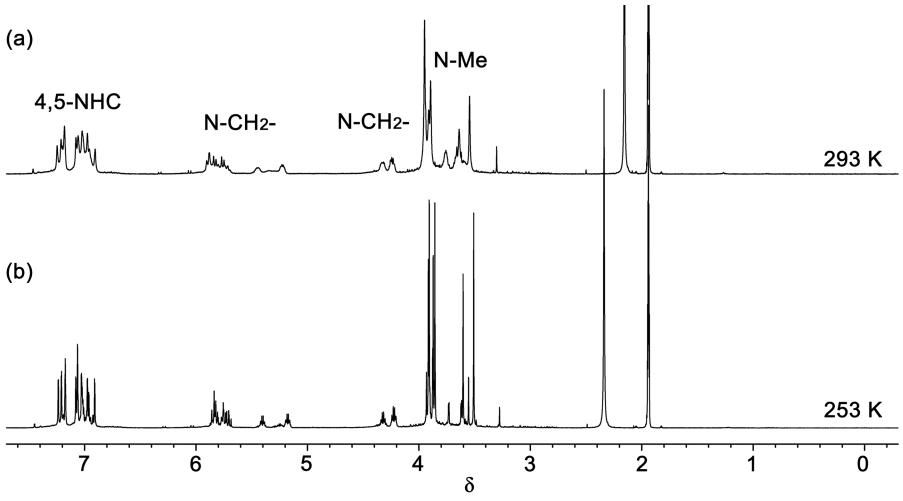

Fig. S2 ^{1}H NMR spectra of mixed-ligand triplatinum complex with two bisNHC-C1 and one bisNHC-C2 ligands, $[\mathbf{Pt}^{\mathbf{C1}}_{\mathbf{2}}\mathbf{Pt}^{\mathbf{C2}}]^{2+}$, (a) at 293 K and (b) at 253 K (600 MHz, CD_3CN). Several sets of sharp signals of the bisNHC ligands were observed at 253 K showing the existence of isomers in solution. The signals at 253 K become broad at 293 K due to the flapping motion of the bisNHC ligands.

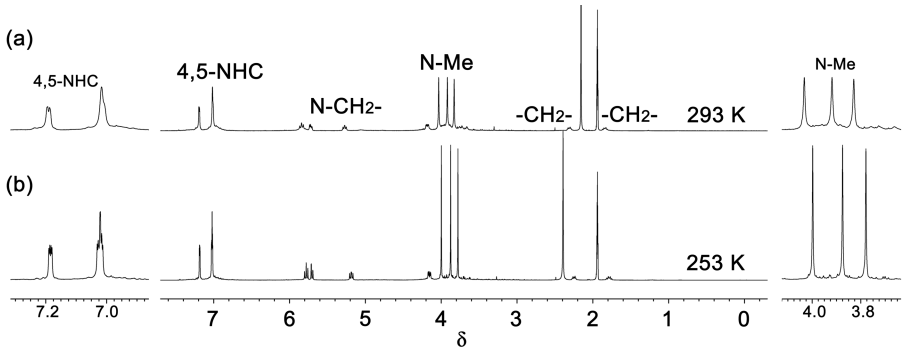

Fig. S3 ^{1}H NMR spectra of mixed-ligand triplatinum complex with two bisNHC-C1 and one bisNHC-C3 ligands, $[\mathbf{Pt^{C1}_2Pt^{C3}}]^{2+}$, (a) at 293 K and (b) at 253 K (600 MHz, CD_3CN). Three sets of signals for the bisNHC ligands were observed both at 253 K and 293 K. The three signals for the N-Me protons of three bisNHC ligands in $[\mathbf{Pt^{C1}_2Pt^{C3}}]^{2+}$ observed at 253 K clearly show the existence of one of the isomers. Three slightly broad signals observed at 293 K suggests the flapping motion and the equilibrium shifts to one of the isomers.

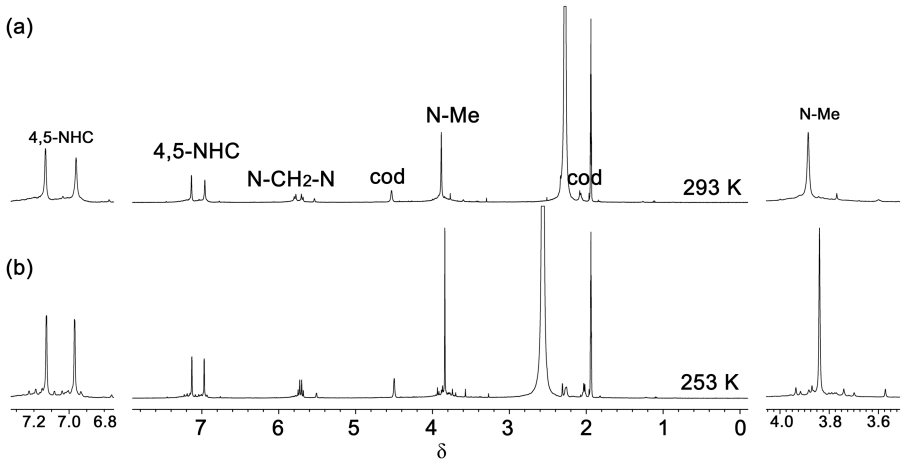

Fig. S4 ^{1}H NMR spectra of mixed-metal complex with two {Pt(bisNHC-C1)} and one {Rh(cod)} moieties, $[\mathbf{Pt^{C1}_2Rh^{cod}}]^{+}$, (a) at 293 K and (b) at 253 K (600 MHz, CD_3CN). One set of signals of the bisNHC ligands was observed at 253 K showing the existence of one of the isomers. One set of slightly broad signals appeared at 295 K. suggesting the dynamic behaviour due to the flapping motion of the bisNHC ligands and the equilibrium among the isomers shifted to one of them.

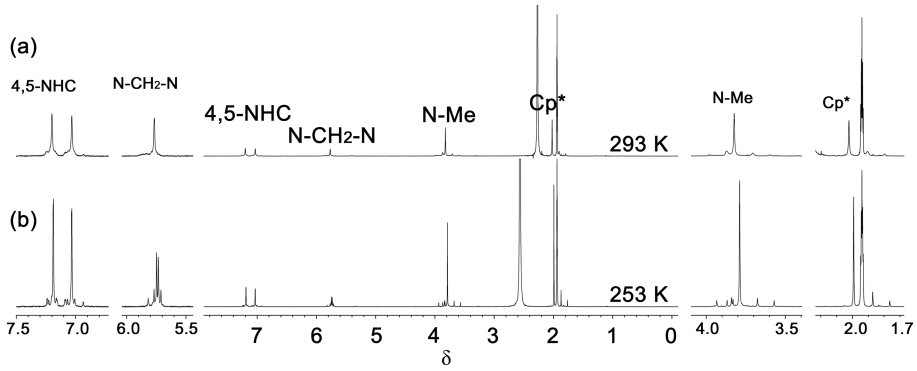

Fig. S5 ^{1}H NMR spectra of mixed-metal complex with two {Pt(bisNHC-C1)} and one {RhCp*} moieties, $[\mathbf{Pt^{C1}_2Rh^{Cp*}}]^{2+}$, (a) at 293 K and (b) at 253 K (600 MHz, CD_3CN). One set of signals of the bisNHC ligands was observed at 253 K showing the existence of one of the isomers. One set of slightly broad signals appeared at 295 K. suggesting the dynamic behaviour due to the flapping motion of the bisNHC ligands and the equilibrium among the isomers shifted to one of them.

2. ^{1}H NMR spectra of the reaction mixtures of the complexes with Ag(I) ions

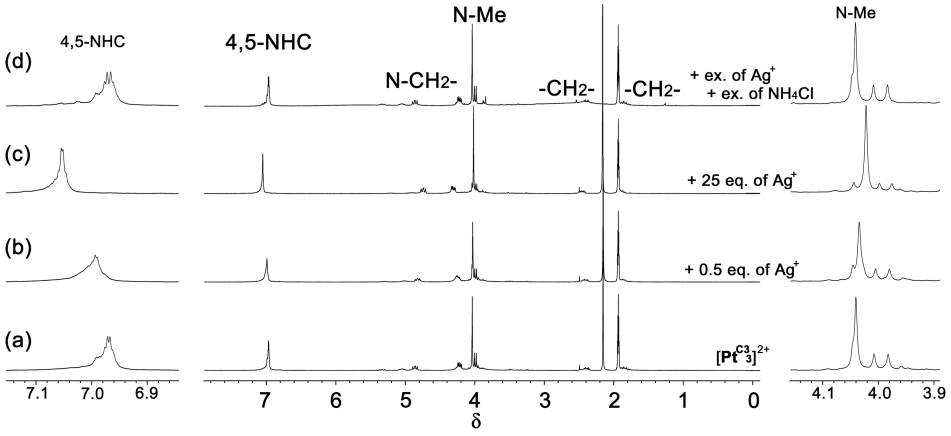

Fig. S6 ^{1}H NMR spectra of (a) triplatinum complex bearing bisNHC-C3 ligands, $[\mathbf{Pt^{C3}_3}]^{2+}$, and its reaction mixtures with (b) 0.5 eq. and (c) 25 eq. of Ag^{+}, and (d) (c)+ex. of NH_4Cl (400 MHz, CD_3CN). Slightly broad signals were observed for $[\mathbf{Pt^{C3}_3}]^{2+}$ and the highest signal observed in the N-Me region is attributed to the symmetric isomer beside the other three are assigned to the unsymmetric one in (a). With the addition of Ag)(I) ions, the highest peak in the N-Me region moves toward the higher magnetic field in (b) and (c) and the intensities of the three small signals for the *C*s isomer decrease. The signals in (d) after the addition of chloride ions to extract the Ag(I) ion are the same as those of the complex in (a).

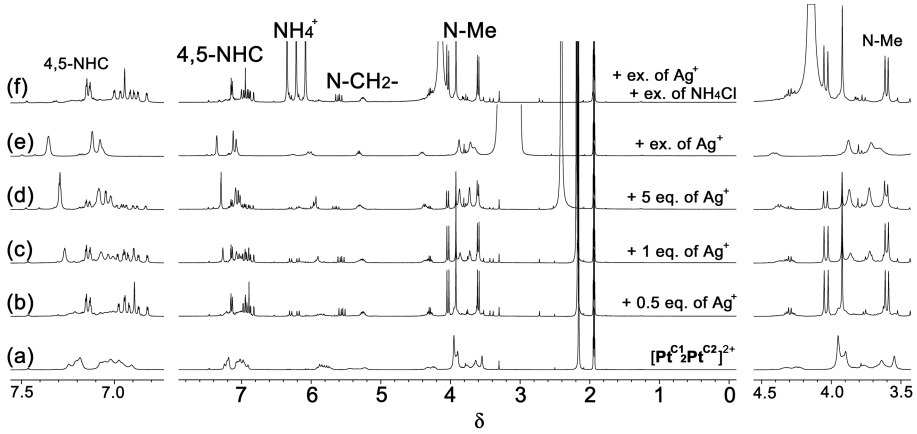

Fig. S7 ^{1}H NMR spectra of (a) triplatinum complex bearing two bisNHC-C1 and one bisNHC-C2 ligands, $[\mathbf{Pt^{C1}_2Pt^{C2}}]^{2+}$, and its reaction mixtures with (b) 0.5 eq., (c) 1 eq., (d) 5 eq., (e) ex. of Ag(I) ions, and (f) (e)+ex. of NH_4Cl (400 MHz, CD_3CN). Broad signals appeared in (a) showing the dynamic behaviour due to the flapping motion of the bisNHC ligands. The signals become sharp after the addition of 0.5 eq. of Ag(I) ions (b). After the further addition of Ag(I) ions, the intensities of the sharp signals decrease, and other broad signals appear in (b)–(d). Only broad signals are observed in (e) after the addition of excess Ag(I) ions. The same spectrum (f) as (b) is obtained after the addition of chloride ions to extract Ag(I) ions.

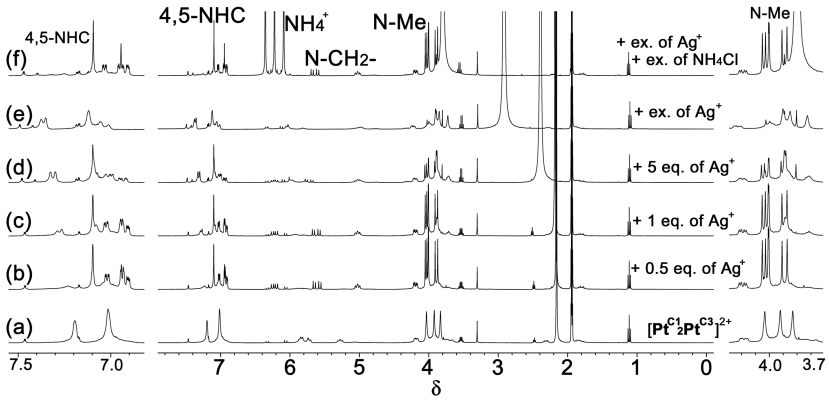

Fig. S8 ^{1}H NMR spectra of (a) triplatinum complex bearing two bisNHC-C1 and one bisNHC-C3 ligands, $[\mathbf{Pt^{C1}_2Pt^{C3}}]^{2+}$, and its reaction mixtures with (b) 0.5 eq., (c) 1 eq., (d) 5 eq., (e) ex. of Ag(I) ions, and (f) (e)+ex. of NH_4Cl (400 MHz, CD_3CN). Three sets of broad signals appeared in (a) showing the dynamic behaviour due to the flapping motion of the bisNHC ligands and the equilibrium shifts to one of the isomers. The signals become sharp after the addition of 0.5 eq. of Ag(I) ions (b). After the further addition of Ag(I) ions, the intensities of the sharp signals decrease, and other broad signals appear in (b)–(d). Only broad signals are observed in (e) after the addition of excess Ag(I) ions. The addition of chloride ions (f) affords the same spectrum as (b).

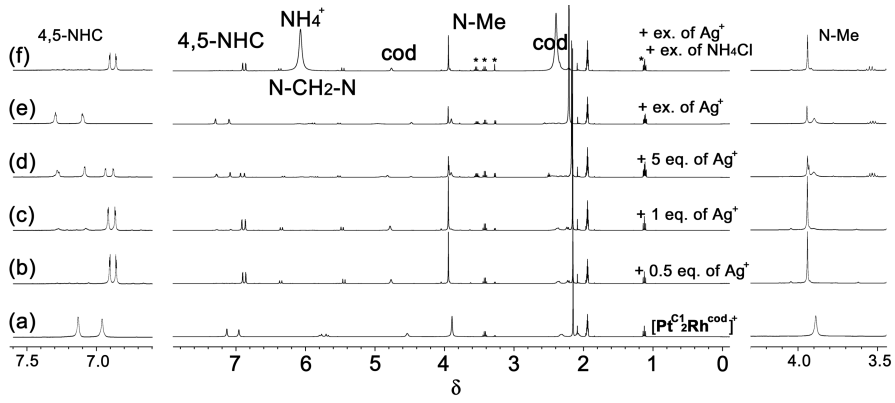

Fig. S9 ^{1}H NMR spectra of (a) trinuclear complex bearing two {Pt(bisNHC-C1)} and one {Rh(cod)} moieties, $[\mathbf{Pt^{C1}_2Rh^{cod}}]^+$, and its reaction mixtures with (b) 0.5 eq., (c) 1 eq., (d) 5 eq., (e) ex. of Ag^+, and (f) (e)+ex. of NH_4Cl (400 MHz, CD_3CN). *Solvents (MeOH, EtOH, Et_2O). One set of the broad signals, which are assigned to the bisNHC ligands one of the isomers, appears in (a). The addition of 0.5 eq. of Ag(I) ions affords one set of the sharp signals in (b) suggesting the formation of the heptanuclear complex. The intensities of the signals decrease after the further addition of Ag(I) ions and another set of signals appears in (c) and (d). In the presence of excess Ag(I) ions, the signals for the heptanuclear complex disappear (e) and only the appeared signals are observed. After the addition of chloride ions, the same signals for the heptanuclear complex (f) as those in (a) are obtained.

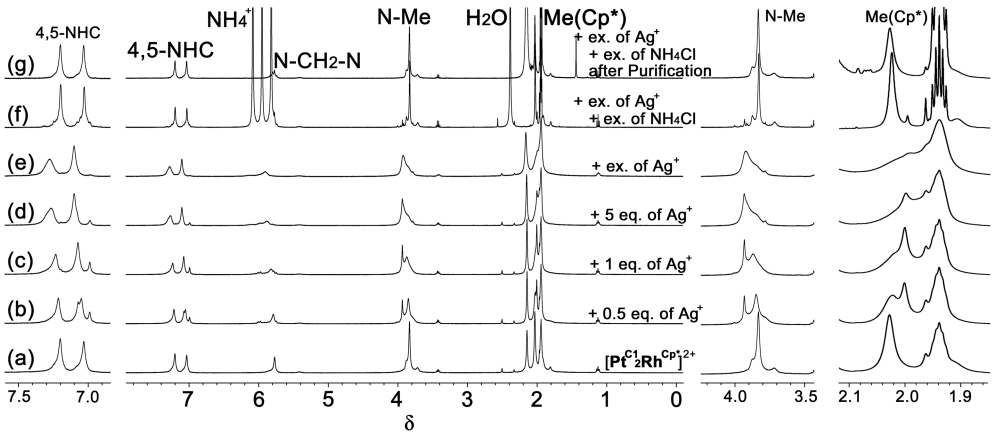

Fig. S10 ^{1}H NMR spectra of (a) trinuclear complex bearing two {Pt(bisNHC-C1)} and one {RhCp} moieties, $[\mathbf{Pt^{C1}_2Rh^{Cp^*}}]^{2+}$, and its reaction mixtures with (b) 0.5 eq., (c) 1 eq., (d) 5 eq., (e) ex. of Ag^+, (f) (e)+ex. of NH_4Cl and (g) (e) after purification to remove NH_4^+ (400 MHz, CD_3CN). After the addition of Ag(I) ions, one set of signals other than those for $[\mathbf{Pt^{C1}_2Rh^{Cp^*}}]^{2+}$ appears in (b) and their intensities increase in (c) and (d). Only the increased signals are observed in the presence of excess Ag(I) ions. The signals for $[\mathbf{Pt^{C1}_2Rh^{Cp^*}}]^{2+}$ are retrieved by the addition of chloride ions to extract Ag(I) ions from the reaction system in (f) and (g).

3. ^{195}Pt NMR spectroscopy

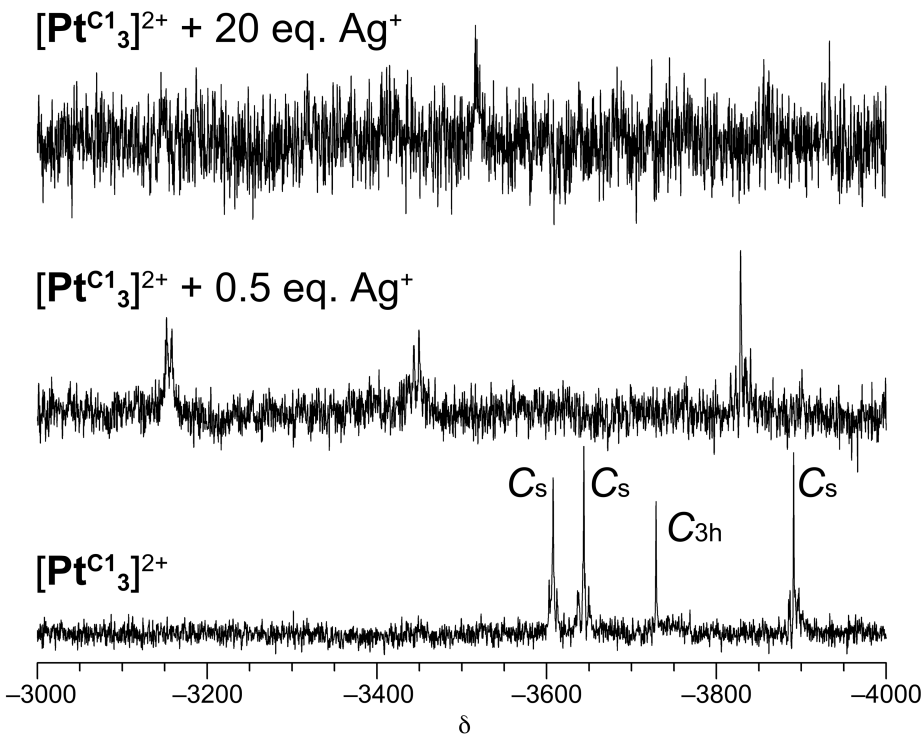

Fig. S11 ^{195}Pt NMR spectra for reactions of $[\mathbf{Pt^{C1}}_3]^{2+}$ and Ag(I) salt in CD_3CN.

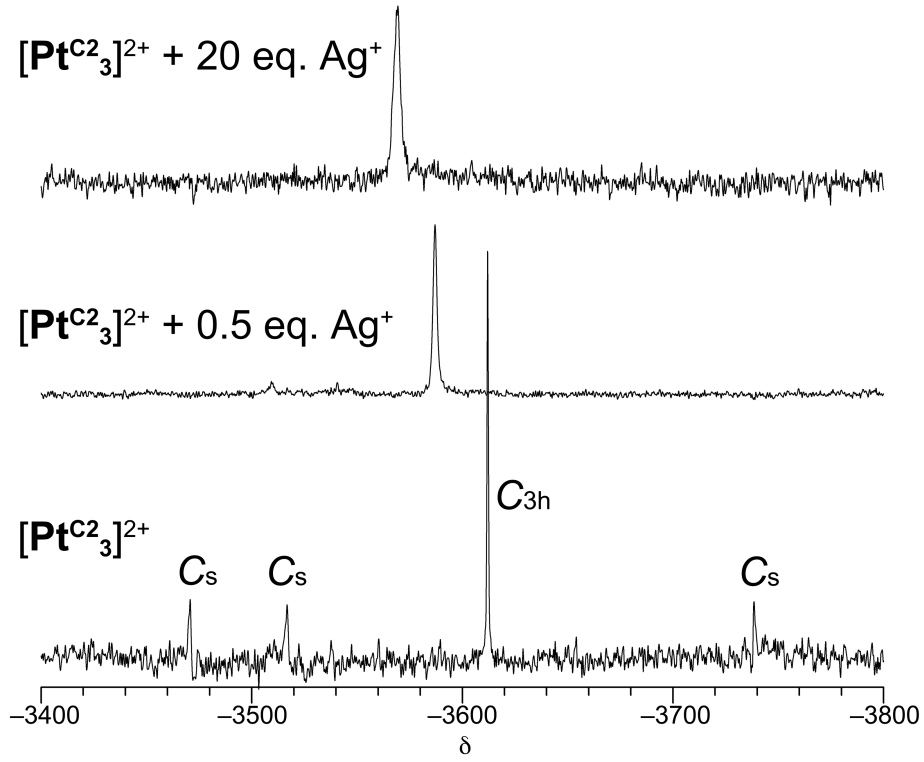

Fig. S12 ^{195}Pt NMR spectra for reactions of $[\mathbf{Pt^{C2}}_3]^{2+}$ and Ag(I) salt in CD_3CN.

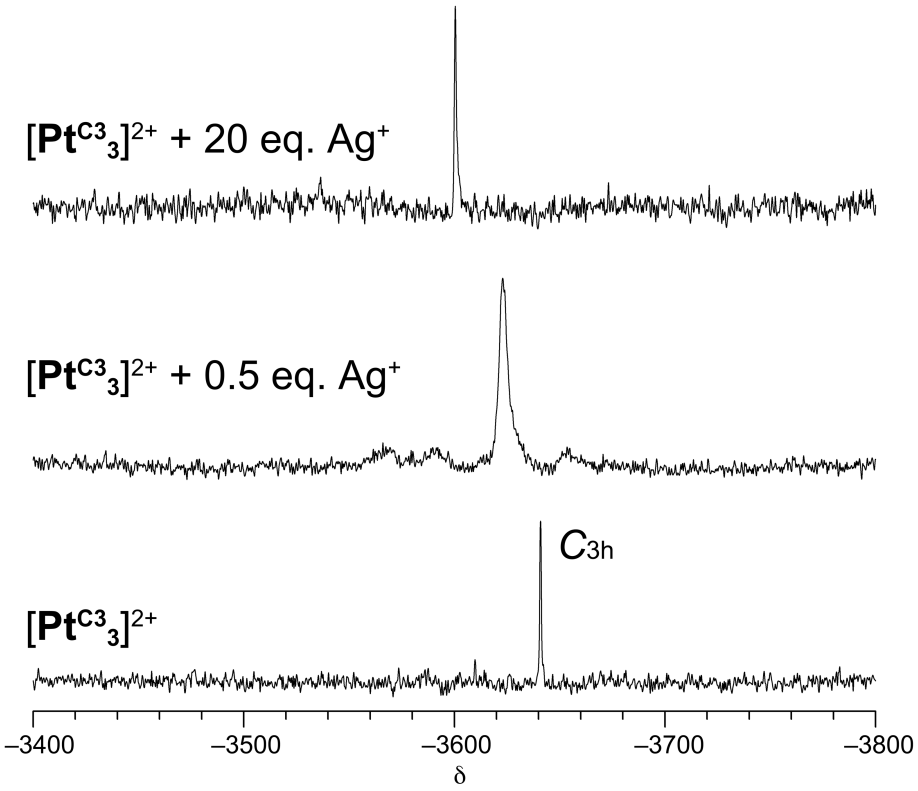

Fig. S13 ^{195}Pt NMR spectra for reactions of $[\mathbf{Pt^{C3}_3}]^{2+}$ and Ag(I) salt in CD_3CN.

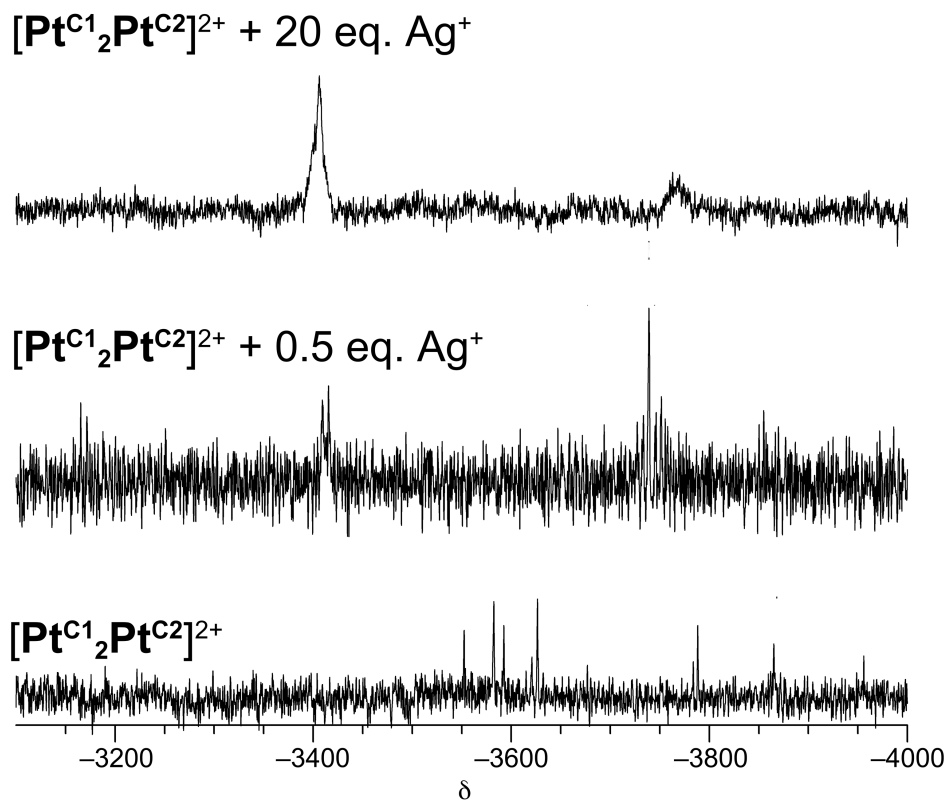

Fig. S14 ^{195}Pt NMR spectra for reactions of $[\mathbf{Pt^{C1}_2Pt^{C2}}]^{2+}$ with Ag(I) salt.

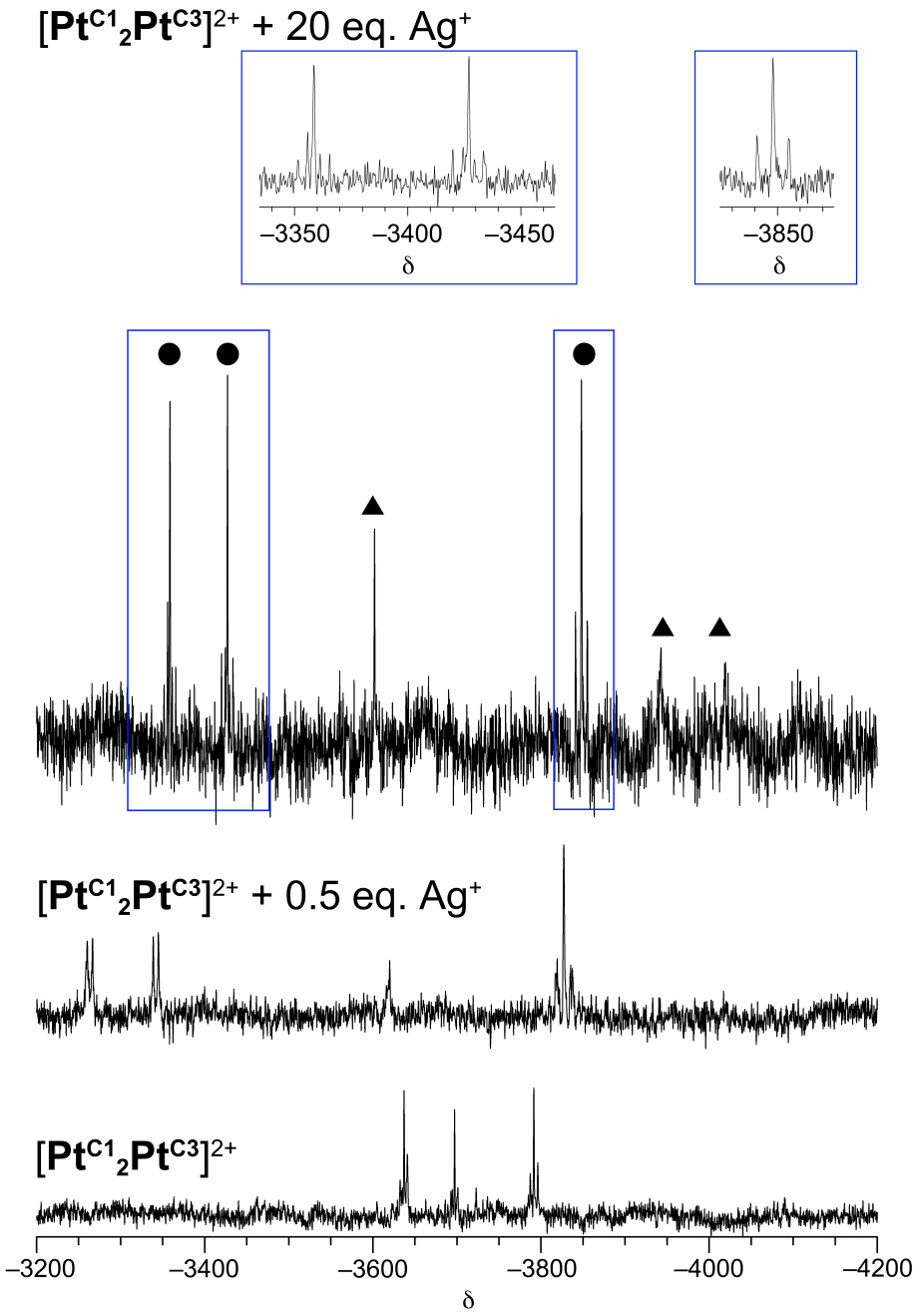

Fig. S15 ^{195}Pt NMR spectra for reactions of $[\mathbf{Pt^{C1}_2Pt^{C3}}]^{2+}$ with Ag(I) salt. The signals classified with black circles or triangles are assigned to each of Ag-adduct.

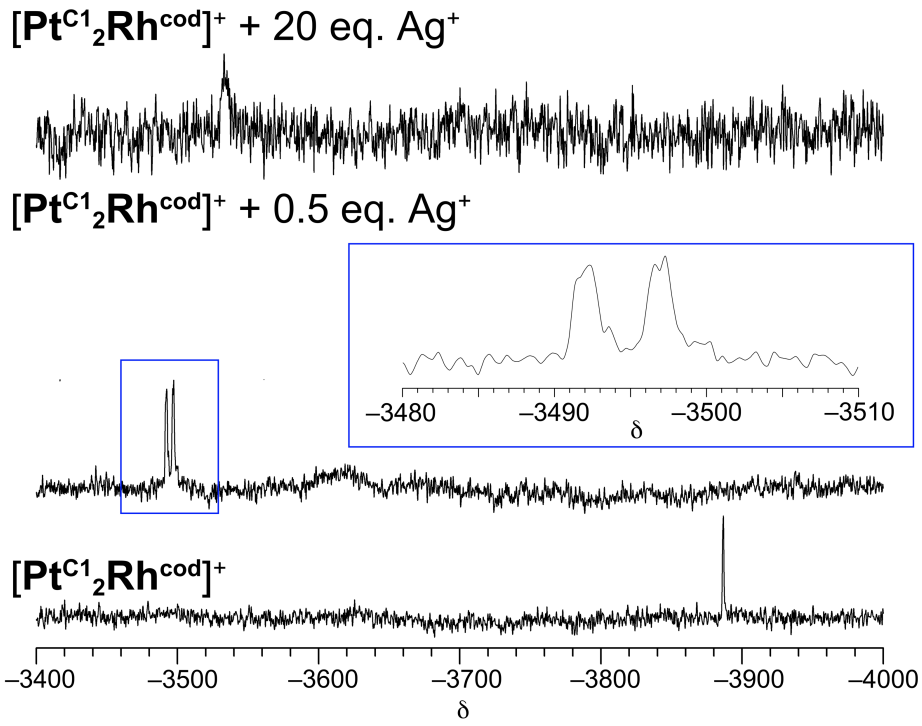

Fig. S16 ^{195}Pt NMR spectra for reactions of [**Pt$^{C1}_2$Rh^{cod}**]$^+$ with Ag(I) salts in CD_3CN.

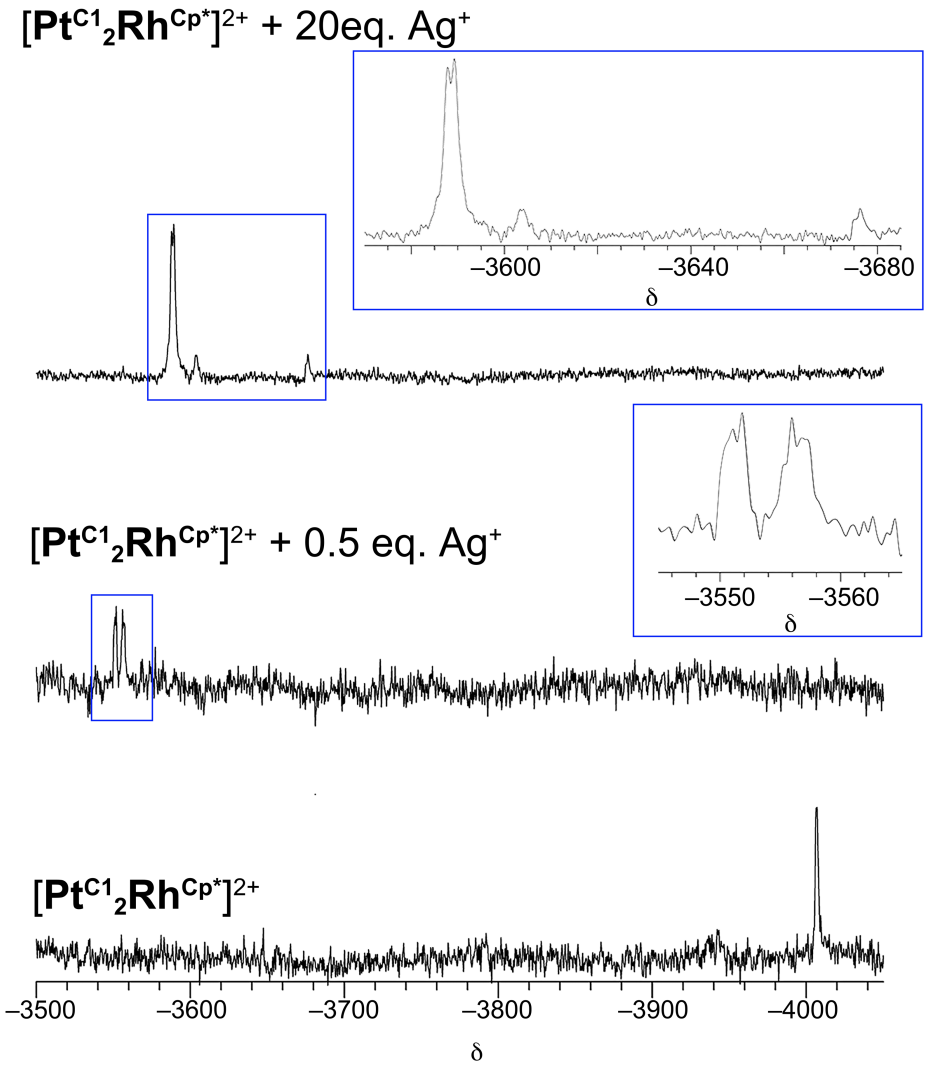

Fig. S17 ^{195}Pt NMR spectra for reactions of $[\mathbf{Pt^{C1}_2Rh^{Cp*}}]^{2+}$ with Ag(I) salts in CD_3CN.

4. X-ray crystallography

Crystallographic data are summarised in Tables S1–S9 for $[\mathbf{Pt^{C2}_3}](PF_6)_2$, $[\mathbf{Pt^{C3}_3}](PF_6)_2$, $[\mathbf{Pt^{C1}_2Pt^{C2}}](PF_6)_2$, $[\mathbf{Pt^{C1}_2Pt^{C3}}](PF_6)_2$, $[\mathbf{Pt^{C1}_2Rh^{Cp^*}}](BPh_4)_2$, $[\mathbf{Pt^{C1}_2Rh^{cod}}](PF_6)$, $[Ag\{[Pt(bisNHC\text{-}C2)]_3[Ag(NCCH_3)_3](\mu_4\text{-}S)_2\}_2](PF_6)_7$, $[\{Pt(bisNHC\text{-}C1)\}_2\{Pt(bisNHC\text{-}C3)\}(\mu_4\text{-}S)_2\{Ag(O_2PF_2)\}\{Ag(NCCH_3)_{0.5}(OCH_3)_{0.5}\}(\mu\text{-}O_2PF_2)](PF_6)_{1.5}$ and $[\{Pt(bisNHC\text{-}C3)\}_3\{Ag(NCCH_3)_3\}_2(\mu_4\text{-}S)_2](PF_6)_4$, respectively. Some of the structures contain positionally disordered atoms as follows.

$[\mathbf{Pt^{C1}_2Pt^{C2}}](PF_6)_2$

Although electron densities attributed to one toluene molecule were found on the difference Fourier map, the toluene molecule in the crystal contained as a solvent for crystallisation was positionally disordered and least square refinement gave distorted structure and large temperature factors for the atoms of the solvent molecules. Because of the difficulty for the sufficient refinement, the solvent mask was applied using PLATON/SQUEEZE.[1]

$[\mathbf{Pt^{C1}_2Pt^{C3}}](PF_6)_2$

Although electron densities attributed to two methanol molecules were found on the difference Fourier map, the molecules in the crystal contained as a solvent for crystallisation were positionally disordered and least square refinement gave distorted structure and large temperature factors for the atoms of the solvent molecules. Because of the difficulty for the sufficient refinement, the solvent mask was applied using PLATON/SQUEEZE.[1] Some of the F atoms in one of two PF_6 anions were treated as positionally disordered.

$[\mathbf{Pt^{C1}_2Rh^{Cp^*}}](BPh_4)_2$

Although electron densities attributed to three dichloromethane molecules were found on the difference Fourier map, the molecules in the crystal contained as a solvent for crystallisation were positionally disordered and least square refinement gave distorted structures and large temperature factors for the atoms of the solvent molecules. Because of the difficulty for the sufficient refinement, the solvent mask was

applied using PLATON/SQUEEZE.[1] The Cp* ligand was also positionally disordered due to the rotation of the ligand. The structure was refined with two orientations of the ligand, which are related to each other by the crystallographic mirror plane.

$[Pt^{C1}{}_2Rh^{cod}](PF_6)$

Although electron densities attributed to two acetonitrile molecules were found on the difference Fourier map, the molecules in the crystal contained as a solvent for crystallisation were positionally disordered and least square refinement gave distorted structures and large temperature factors for the atoms of the solvent molecules. Because of the difficulty for the sufficient refinement, the solvent mask was applied using SQUEEZE.[1] The cod ligand was also positionally disordered due to the mismatch of the cod ligand and the crystallographic *C*2 axis. The structure was refined with two orientations of the ligand, which are related to each other by the crystallographic *C*2 axis in the complex cation. Some of the F atoms in the PF_6 anion were also treated as positionally disordered.

$[\{Pt(bisNHC\text{-}C1)\}_2\{Pt(bisNHC\text{-}C3)\}(\mu_4\text{-}S)_2[\{Ag(O_2PF_2)\}\{Ag(NCCH_3)_{0.5}(OCH_3)_{0.5})\}(\mu\text{-}O_2PF_2)](PF_6)_{1.5}$

Although electron densities attributed to acetonitrile and methanol molecules were found on the difference Fourier map, the molecules in the crystal contained as a solvent for crystallisation were positionally disordered and least square refinement gave distorted structures and large temperature factors for the atoms of the solvent molecules. Because of the difficulty for the sufficient refinement, the solvent mask was applied using PLATON/SQUEEZE.[1] One water molecule was excluded the SQUEEZE calculation and its O atom was included in the refinement of the structure model. The F and O atoms of the bridging difluorophosphate ligands were treated with two orientations of the ligand. One of the two terminal ligands for Ag(I) ions was also disordered with acetonitrile and methoxy ligands in 1:1 ratio. The result of the analysis showed that the crystal contains 1.5 eq. of PF_6 anions meaning the pentanuclear complex has 1.5

positive charge. This strange positive charge is attributed to the disordered terminal ligand of Ag(I), which is a 1: 1 mixture of neutral acetonitrile and methoxy monoanion.

Supplemental data of crystallographic analysis for [{Pt(bisNHC-C3)}$_3${Ag(NCCH$_3$)$_3$}$_2$(μ_4-S)$_2$](PF$_6$)$_4$

The PF_6 anions are disordered and then some of the fluorine atoms could not be found in the difference Fourier maps. In the asymmetric unit, there are one and a half of the pentanuclear units. One of the two independent complex cations, which has a two-fold axis, exhibited huge disorder for the bisNHC ligands due to the crystallographic symmetry and insufficient quality of the crystal. The other showed the C_{3h}-isomeric form of the triplatinum unit as shown in the main text of the article. Although this analysis is not suitable for discussion about the detail of the structure, the obtained framework of the complex dication clearly indicate the formation of the Ag-adduct containing two Ag–S bonds with both of the sulfide ligands in the triplatinum complex along with the C_{3h}-isomeric form of the triplatinum unit in the adduct.

Table S1. Crystallographic data of triplatinum complex [$\mathbf{Pt^{C^2}_3}$]$(PF_6)_2$ (CCDC 2238719).

Formula	$C_{30}H_{42}F_{12}N_{12}P_2Pt_3S_2$
M_w	1510.06
Crystal description	colourless, prism
Crystal size/mm	0.138 × 0.073 × 0.067
Crystal system	*monoclinic*
Space group	$P2_1/c$ (#14)
a/Å	15.4330(11)
b/Å	15.7491(19)
c/Å	19.3229(15)
α/°	90
β/°	91.050(3)
γ/°	90
V/Å^3	4695.8(8)
Z	4
F(000)	2840.00
ρ_{calcd}/g cm^{-1}	2.136
μ/mm^{-1}	9.122
Total reflections	47348
Unique reflections (R_{int})	21456 (0.0457)
Scan range θ/°	27.445
Completeness	0.997
Index ranges	–19≤ h ≤ 19
	–20 ≤ k ≤ 19
	–25 ≤ l ≤ 24
Data/restrains/para.	10693/0/589
$R1$ [I>2σ(I)], $wR2$ (all data)	0.0513, 0.1073
GOF on F^2	1.002
Max./min. ρ/eÅ^{-3}	2.40/–2.07
Min./max. T	0.325/0.543

Table S2. Crystallographic data of triplatinum complex [$\mathbf{Pt^{C3}_3}$]$(PF_6)_2$•CH_3CN (CCDC 2238720).

Formula	$C_{39}H_{57}F_{12}N_{15}P_2Pt_3S_2$
M_w	1675.28
Crystal description	colourless, prism
Crystal size/mm	0.15 × 0.12 × 0.11
Crystal system	*hexagonal*
Space group	$P6_3/m$ (#176)
a/Å	14.1996(6)
b/Å	= a
c/Å	16.3484(7)
α/°	90
β/°	90
γ/°	120
V/Å^3	2854.7(2)
Z	2
F(000)	1600.00
ρ_{calcd}/g cm^{-1}	1.949
μ/mm^{-1}	7.542
Total reflections	95400
Unique reflections (R_{int})	29775 (0.0442)
Scan range θ/°	27.495
Completeness	0.997
Index ranges	–18≤ h ≤ 17
	–18 ≤ k ≤ 18
	–21 ≤ l ≤ 21
Data/restrains/para.	2264/0/119
$R1$ [I>2σ(I)], $wR2$ (all data)	0.0328, 0.0653
GOF on F^2	1.028
Max./min. ρ/eÅ^{-3}	2.33/–1.12
Min./max. T	0.270/0.444

Table S3. Crystallographic data of triplatinum complex [$\mathbf{Pt^{C1}_2Pt^{C2}}$]$(PF_6)_2$•0.5toluene (CCDC 2238721).

Formula	$C_{31.5}H_{42}F_{12}N_{12}P_2Pt_3S_2$
M_w	1528.08
Crystal description	colourless, prism
Crystal size/mm	0.010 × 0.007 × 0.006
Crystal system	*triclinic*
Space group	$P\bar{1}$ (#2)
a/Å	10.2266(3)
b/Å	13.0170(8)
c/Å	16.8232(11)
α/°	99.891(4)
β/°	93.302(3)
γ/°	90.379(2)
V/Å^3	2202.2(2)
Z	2
F(000)	1438.00
ρ_{calcd}/g cm^{-1}	2.304
μ/mm^{-1}	9.765
Total reflections	30075
Unique reflections (R_{int})	9933 (0.0265)
Scan range θ/°	27.450
Completeness	0.991
Index ranges	–13≤ h ≤ 13
	–16 ≤ k ≤ 16
	–21 ≤ l ≤ 21
Data/restrains/para.	9933/0/538
*R*1 [*I*>2σ(*I*)], *wR*2 (all data)	0.0248, 0.0585
GOF on F^2	1.119
Max./min. ρ/eÅ^{-3}	2.596/–0.998
Min./max. *T*	0.624/0.943

Table S4. Crystallographic data of triplatinum complex [$\mathbf{Pt^{C1}_2Pt^{C3}}$]$(PF_6)_2$•1.5$CH_3OH$ (CCDC 2238722).

Formula	$C_{30.5}H_{46}F_{12}N_{12}O_{1.5}P_2Pt_3S_2$
M_w	1544.12
Crystal description	colourless, prism
Crystal size/mm	0.139 × 0.124 × 0.041
Crystal system	*triclinic*
Space group	$P\bar{1}$ (#2)
a/Å	12.4809(2)
b/Å	14.6151(5)
c/Å	15.70520(10)
α/°	77.649(18)
β/°	66.585(13)
γ/°	77.483(17)
V/Å^3	2540.2(3)
Z	2
F(000)	1458.00
ρ_{calcd}/g cm^{-1}	2.019
μ/mm^{-1}	8.469
Total reflections	32367
Unique reflections (R_{int})	11397 (0.0347)
Scan range θ/°	27.407
Completeness	0.984
Index ranges	–16≤ h ≤ 16
	–18 ≤ k ≤ 18
	–20 ≤ l ≤ 20
Data/restrains/para.	11397/0/547
*R*1 [*I*>2σ(*I*)], *wR*2 (all data)	0.0384, 0.0938
GOF on F^2	1.062
Max./min. ρ/eÅ^{-3}	3.058/–3.280
Min./max. *T*	0.536/0.708

Table S5. Crystallographic data of diplatinum rhodium complex [$\mathbf{Pt^{C1}_2Rh^{Cp^*}}$]$(BPh_4)_2$ (CCDC 2238723).

Formula	$C_{79}H_{85}B_2Cl_6N_8Pt_2RhS_2$
M_w	1938.17
Crystal description	green, plate
Crystal size/mm	0.170 × 0.040 × 0.020
Crystal system	*monoclinic*
Space group	*Cm* (#8)
a/Å	17.827(4)
b/Å	25.802(4)
c/Å	13.476(3)
α/°	90
β/°	128.641(5)
γ/°	90
V/Å^3	4841.6(18)
Z	2
F(000)	1920
ρ_{calcd}/g cm^{-1}	1.329
μ/mm^{-1}	3.298
Total reflections	29802
Unique reflections (R_{int})	9154 (0.0606)
Scan range θ/°	25.50
Completeness	0.997
Index ranges	–22≤ h ≤ 22
	–33 ≤ k ≤ 33
	–17 ≤ l ≤ 17
Data/restrains/para.	9154/365/412
*R*1 [*I*>2σ(*I*)], *wR*2 (all data)	0.0399, 0.1020
GOF on F^2	0.8978
Max./min. ρ/eÅ^{-3}	1.342/–1.250
Min./max. *T*	0.574/0.936

Table S6. Crystallographic data of diplatinum rhodium complex [$\mathbf{Pt^{C1}_2Rh^{cod}}$]($PF_6$)•2$CH_3CN$ (CCDC 2238724).

Formula	$C_{30}H_{42}F_6N_{10}PPt_2RhS_2$
M_w	1285.95
Crystal description	yellow, prism
Crystal size/mm	0.143 × 0.089 × 0.031
Crystal system	*tetragonal*
Space group	$I4_1$ (#80)
a/Å	12.3687(11)
b/Å	= *a*
c/Å	27.8127(18)
α/°	90
β/°	90
γ/°	90
V/Å^3	4254.9(6)
Z	4
F(000)	2376.00
ρ_{calcd}/g cm^{-1}	2.007
μ/mm^{-1}	7.141
Total reflections	21520
Unique reflections (R_{int})	4875 (0.0534)
Scan range θ/°	27.489
Completeness	0.997
Index ranges	–16≤ h ≤ 16
	–16 ≤ k ≤ 16
	–36 ≤ l ≤ 35
Data/restrains/para.	4875/290/263
*R*1 [*I*>2σ(*I*)], *wR*2 (all data)	0.0492, 0.1169
GOF on F^2	1.006
Max./min. ρ/eÅ^{-3}	1.801/–2.219
Min./max. *T*	0.596/0.802
Flack parameter	0.042(6)

Table S7. Crystallographic data of Ag-adduct $[Ag\{[Pt(bisNHC\text{-}C2)]_3[Ag(NCCH_3)_3](\mu_4\text{-}S)_2\}_2](PF_6)_7$ (CCDC 2238725).

Formula	$C_{72}H_{102}Ag_3F_{42}N_{30}P_7Pt_6S_4$
M_w	4024.93
Crystal description	colourless, prism
Crystal size/mm	0.196 × 0.063 × 0.010
Crystal system	*triclinic*
Space group	$P\bar{1}$ (#2)
a/Å	16.814(7)
b/Å	17.820(7)
c/Å	22.082(9)
α/°	101.846(7)
β/°	92.738(12)
γ/°	92.657(5)
V/Å^3	6458(5)
Z	2
F(000)	3800.00
ρ_{calcd}/g cm^{-1}	2.070
μ/mm^{-1}	7.149
Total reflections	66567
Unique reflections (R_{int})	29011 (0.0486)
Scan range θ/°	27.478
Completeness	0.980
Index ranges	–21≤ h ≤ 21
	–22 ≤ k ≤ 23
	–26 ≤ l ≤ 28
Data/restrains/para.	29011/0/1483
*R*1 [*I*>2σ(*I*)], *wR*2 (all data)	0.0625, 0.1643
GOF on F^2	1.016
Max./min. ρ/eÅ^{-3}	3.22/–2.40
Min./max. *T*	0.628/0.931

Table S8. Crystallographic data of Ag-adduct [{Pt(bisNHC-C1)}$_2${Pt(bisNHC-C3)}(μ_4-S)$_2${Ag(O_2PF_2)}{Ag($NCCH_3$)$_{0.5}$(OCH_3)$_{0.5}$}(μ-O_2PF_2)](PF_6)$_{1.5}$•CH_3CN•CH_3OH•H_2O (CCDC 2238726).

Formula	$C_{33.5}H_{52}Ag_2F_{13}N_{13.5}O_{6.5}P_{3.5}Pt_3S_2$
M_w	2015.22
Crystal description	colourless, platelet
Crystal size/mm	0.204 × 0.038 × 0.012
Crystal system	*monoclinic*
Space group	$P2_1/c$ (#14)
a/Å	24.235(2)
b/Å	12.8335(9)
c/Å	20.6397(18)
α/°	90
β/°	112.905(2)
γ/°	90
V/Å^3	5913.2(8)
Z	4
F(000)	3702.00
ρ_{calcd}/g cm^{-1}	2.264
μ/mm^{-1}	7.982
Total reflections	59421
Unique reflections (R_{int})	13383 (0.0547)
Scan range θ/°	27.402
Completeness	0.994
Index ranges	–31≤ h ≤ 31
	–16 ≤ k ≤ 16
	–26 ≤ l ≤ 26
Data/restrains/para.	13383/56/660
*R*1 [*I*>2σ(*I*)], *wR*2 (all data)	0.0684, 0.1283
GOF on F^2	1.039
Max./min. ρ/eÅ^{-3}	2.382 /–2.865
Min./max. *T*	0.687/0.909

Table S9. Preliminary crystallographic data of Ag-adduct $[\{Pt(bisNHC\text{-}C3)\}_3\{Ag(NCCH_3)_3\}_2(\mu_4\text{-}S)_2](PF_6)_4$.

Formula	$C_{45}H_{66}AgF_{24}N_{18}P_4Pt_3S_2$
M_w	1362.57
Crystal description	colourless, prism
Crystal size/mm	0.174 × 0.075 × 0.070
Crystal system	*orthorhombic*
Space group	*Pbcn* (#60)
a/Å	43.897(18)
b/Å	25.323(11)
c/Å	25.885(11)
α/°	90
β/°	90
γ/°	90
V/Å^3	28773(21)
Z	12
F(000)	13176.00
ρ_{calcd}/g cm^{-1}	1.596
μ/mm^{-1}	4.935
Total reflections	134995
Unique reflections (R_{int})	30075 (0.0722)
Scan range θ/°	26.940
Completeness	0.964
Index ranges	–55≤ h ≤ 47
	–30 ≤ k ≤ 28
	–32 ≤ l ≤ 32
Data/restrains/para.	30075/0/649
*R*1 [*I*>2σ(*I*)], *wR*2 (all data)	0.0651, 0.1813
GOF on F^2	1.095
Max./min. ρ/eÅ^{-3}	10.10/–6.68
Min./max. *T*	0.511/0.708

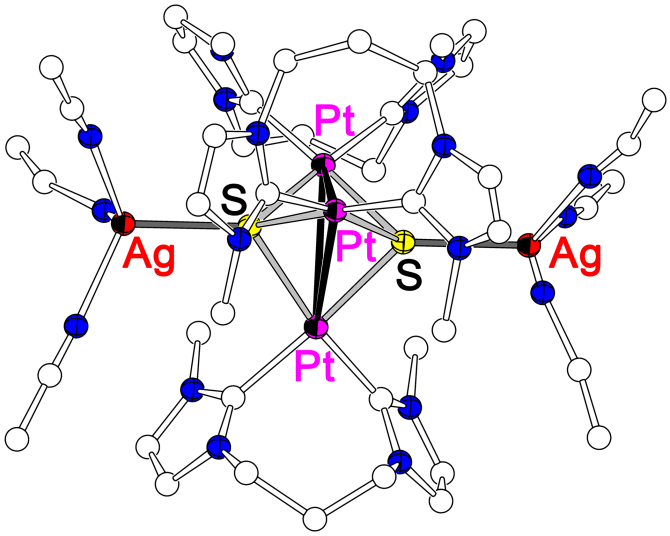

Fig. S18 Supplementary data for structure of pentanuclear Ag-adduct of triplatinum complex bearing three bisNHC-C3 ligands.

5. DFT calculations

Table S10. Optimised atomic coordinates of triplatinum complex $[\mathbf{Pt^{C1}_2Rh^{Cp^*}}]^{2+}$ obtained from DFT calculations.

Number	atom	x	y	z
1	Pt	1.637181	–0.667715	0.002490
2	Pt	–1.706967	–0.551709	0.002792
3	Rh	0.105700	2.157372	–0.003892
4	S	–0.000588	0.328573	1.597454
5	S	–0.000404	0.323096	–1.595207
6	N	3.367659	–2.784447	1.199640
7	N	3.368461	–1.098487	2.578258
8	N	3.356043	–2.790970	–1.199707
9	N	3.343376	–1.110035	–2.584516
10	N	–3.581106	–2.537496	1.208386
11	N	–3.453785	–0.853420	2.583679
12	N	–3.582000	–2.543680	–1.190616
13	N	–3.457102	–0.865738	–2.573580
14	C	2.844136	–1.515928	1.380081
15	C	4.200030	–3.151979	2.269485
16	C	4.193498	–2.092749	3.136558
17	C	3.153120	0.210721	3.217586
18	C	3.067971	–3.577181	0.003666
19	C	2.832939	–1.522663	–1.378930
20	C	4.174091	–3.164426	–2.278459
21	C	4.158668	–2.108356	–3.149671
22	C	3.108823	0.194096	–3.227734
23	C	–0.361699	4.089113	1.103234
24	C	0.019384	4.064969	–1.247974
25	C	–2.968294	–1.316586	–1.372426
26	C	–4.434110	–2.853794	–2.263181
27	C	–4.348423	–1.800271	–3.133037

28	C	–3.144526	0.422924	–3.214509
29	C	–3.348938	–3.350266	0.010890
30	C	–2.967006	–1.309610	1.383733
31	C	–4.431562	–2.842719	2.283676
32	C	–4.344373	–1.785314	3.148632
33	C	–3.139559	0.437385	3.219711
34	C	1.050956	4.013815	0.887684
35	C	1.289835	3.977972	–0.573400
36	C	–1.011685	4.066086	–0.218223
37	C	2.123709	4.071510	1.934938
38	C	–1.064186	4.241126	2.421640
39	C	–0.204230	4.185659	–2.728375
40	C	–2.486026	4.192404	–0.454141
41	C	2.643946	3.988283	–1.217078
42	H	4.705566	–4.102193	2.327810
43	H	4.698411	–1.962412	4.079931
44	H	2.566939	0.090809	4.134014
45	H	2.606436	0.855136	2.530737
46	H	4.120854	0.662297	3.459200
47	H	3.677698	–4.482933	0.003264
48	H	2.008680	–3.851561	0.009389
49	H	4.678318	–4.115192	–2.338746
50	H	4.652323	–1.982977	–4.099595
51	H	4.053202	0.572702	–3.630869
52	H	2.720876	0.891575	–2.485894
53	H	2.378046	0.093423	–4.035984
54	H	–5.006760	–3.765153	–2.320912
55	H	–4.839163	–1.637074	–4.078753
56	H	–2.591412	1.043950	–2.510757
57	H	–4.076004	0.923681	–3.497463
58	H	–2.529659	0.262869	–4.105609
59	H	–4.027954	–4.205421	0.013360
60	H	–2.315023	–3.708285	0.011439
61	H	–5.004171	–3.753766	2.346459
62	H	–4.833527	–1.617754	4.094408
63	H	–2.581588	1.053697	2.515922
64	H	–2.528216	0.279462	4.113593
65	H	–4.070411	0.942343	3.497326
66	H	1.762121	3.720040	2.905913
67	H	2.464861	5.108931	2.066144
68	H	2.999327	3.476503	1.654853
69	H	–0.524700	3.740570	3.231628
70	H	–2.080756	3.836426	2.389381
71	H	–1.145775	5.305425	2.685536
72	H	–2.779344	3.801321	–1.432665
73	H	–2.774606	5.254107	–0.424243
74	H	–3.069213	3.674316	0.313380
75	H	0.586884	3.693680	–3.302313
76	H	–0.219987	5.244077	–3.025016
77	H	–1.158540	3.745259	–3.033429
78	H	2.604541	3.647474	–2.255789
79	H	3.359642	3.363003	–0.672813
80	H	3.045011	5.012852	–1.222765

Table S11. Optimised atomic coordinates of triplatinum complex $[\mathbf{Pt^{C1}_2Rh^{cod}}]^+$ obtained from DFT calculations.

Number	atom	x	y	z
1	Pt	1.682984	–0.536633	–0.006634
2	Pt	–1.682964	–0.536636	0.006574
3	Rh	0.000075	2.268159	0.000379
4	S	0.005122	0.342271	1.593698
5	S	–0.005141	0.342792	–1.593494
6	N	3.575866	–2.515301	1.180005
7	N	3.441175	–0.838571	2.564517
8	N	3.568509	–2.505399	–1.221672
9	N	3.425224	–0.815943	–2.589945
10	N	–3.568408	–2.506070	1.220648
11	N	–3.425241	–0.817314	2.589798
12	N	–3.575871	–2.514722	–1.181030
13	N	–3.441410	–0.837093	–2.564480
14	C	2.943765	–1.293822	1.365954
15	C	4.444519	–2.812714	2.243297
16	C	4.351109	–1.759934	3.114435
17	C	3.111988	0.451034	3.194532
18	C	3.333654	–3.315189	–0.023472
19	C	2.935112	–1.282596	–1.392841
20	C	4.430990	–2.792783	–2.292753
21	C	4.332140	–1.732007	–3.153577
22	C	3.091934	0.479375	–3.206461
23	C	–0.658427	3.836478	1.398138
24	C	–0.753773	3.705265	–1.454167
25	C	–2.943813	–1.293120	–1.366301
26	C	–4.444646	–2.811477	–2.244395
27	C	–4.351401	–1.758120	–3.114866
28	C	–3.112092	0.452870	–3.193701
29	C	–3.333503	–3.315211	0.022026
30	C	–2.935027	–1.283327	1.392489
31	C	–4.430946	–2.794018	2.291521
32	C	–4.332224	–1.733661	3.152870
33	C	–3.092163	0.477727	3.207014
34	C	–1.393583	4.978799	0.689475
35	C	0.753873	3.705131	1.455012
36	C	0.658521	3.836572	–1.397292
37	C	–1.765471	4.626464	–0.780305
38	C	1.393605	4.978838	–0.688459
39	C	1.765504	4.626359	0.781212
40	H	5.030297	–3.715942	2.295247
41	H	4.847114	–1.589813	4.056060
42	H	2.461399	0.296636	4.060961
43	H	2.585228	1.071082	2.469632
44	H	4.035570	0.949272	3.508132
45	H	4.001237	–4.180016	–0.029023
46	H	2.292537	–3.653792	–0.021689
47	H	5.016660	–3.695318	–2.356520
48	H	4.822429	–1.553173	–4.096577
49	H	4.013484	0.977944	–3.525459
50	H	2.573801	1.095440	–2.471847
51	H	2.432526	0.332773	–4.067515
52	H	–5.030449	–3.714661	–2.296841
53	H	–4.847543	–1.587415	–4.056311
54	H	–2.587823	1.073525	–2.467494

55	H	–4.035477	0.950046	–3.509533
56	H	–2.459192	0.299245	–4.058521
57	H	–4.000936	–4.180155	0.027162
58	H	–2.292327	–3.653625	0.020007
59	H	–5.016582	–3.696609	2.354821
60	H	–4.822613	–1.555286	4.095906
61	H	–2.572448	1.093547	2.473328
62	H	–2.434269	0.330583	4.069139
63	H	–4.013913	0.976850	3.524588
64	H	2.736017	4.112204	0.786812
65	H	1.898750	5.550554	1.369563
66	H	1.155780	3.115720	2.280271
67	H	–1.226679	3.322832	2.173759
68	H	–0.781132	5.888179	0.717331
69	H	–2.312802	5.213526	1.241448
70	H	–2.735977	4.112293	–0.785996
71	H	–1.898712	5.550749	–1.368519
72	H	–1.155702	3.115849	–2.279406
73	H	1.226751	3.323127	–2.173073
74	H	0.780936	5.888086	–0.716222
75	H	2.312743	5.213835	–1.240460

6. ^{1}H and ^{13}C NMR spectroscopy

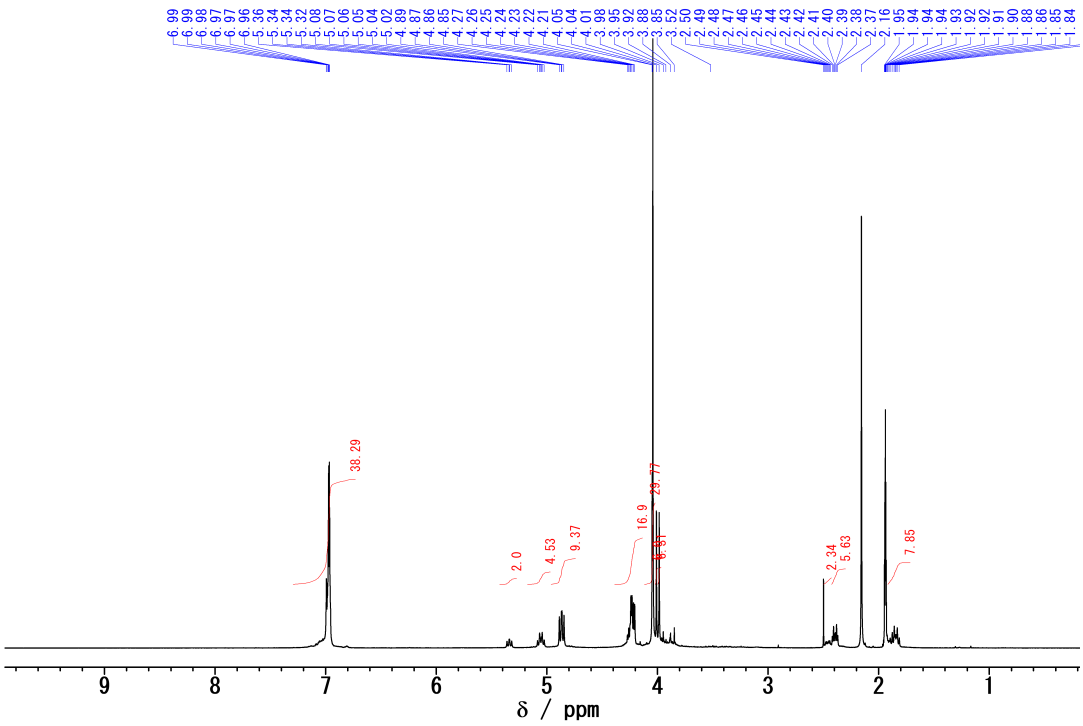

Fig. S19 ^{1}H NMR spectrum of [$\mathbf{Pt^{C3}_3}$](PF$_6$)$_2$ (CD$_3$CN, 600 MHz, 293 K):

C_{3h}-isomer: δ 6.99–9.96 (m, 4,5-im), 4.87 (dd, $^{2}J_{H\text{-}H}$ = 14.3 Hz, $^{3}J_{H\text{-}H}$ = 10.9 Hz, 6H, N-CH$_2$-), 4.22 (dd, $^{2}J_{H\text{-}H}$ = 14.2 Hz, $^{3}J_{H\text{-}H}$ = 6.4 Hz, 6H, N-CH$_2$-), 4.04 (s, 18H, N-Me), 2.39 (ddd, $^{2}J_{H\text{-}H}$ = 13.3 Hz, $^{3}J_{H\text{-}H}$ = 6.7 Hz, $^{3}J_{H\text{-}H}$ = 6.7 Hz, 3H, -CH$_2$-), 1.85 (ddd, $^{2}J_{H\text{-}H}$ = 16.3 Hz, $^{3}J_{H\text{-}H}$ = 10.8 Hz, $^{3}J_{H\text{-}H}$ = 10.8 Hz , 3H, -CH$_2$-).

C_s-isomer: δ 6.99–9.96 (m, 4,5-im), 5.34 (dd, $^{2}J_{H\text{-}H}$ = 14.1 Hz, $^{3}J_{H\text{-}H}$ = 11.6 Hz, 2H, N-CH$_2$-), 5.05 (ddd, $^{2}J_{H\text{-}H}$ = 14.2 Hz, $^{3}J_{H\text{-}H}$ = 11.0 Hz, $^{3}J_{H\text{-}H}$ = 11.0 Hz, 4H, N-CH$_2$-), 4.25 (dd, $^{2}J_{H\text{-}H}$ = 14.1 Hz, $^{3}J_{H\text{-}H}$ = 6.9 Hz, 6H, N-CH$_2$-), 4.05 (s, 6H, N-Me), 4.01 (s, 6H, N-Me), 3.98 (s, 6H, N-Me), 2.46 (ddd, $^{2}J_{H\text{-}H}$ = 16.5 Hz, $^{3}J_{H\text{-}H}$ = 11.1 Hz, $^{3}J_{H\text{-}H}$ = 5.6 Hz ,, 3H, -CH$_2$-), 1.90–1.92 (m, 3H, -CH$_2$-).

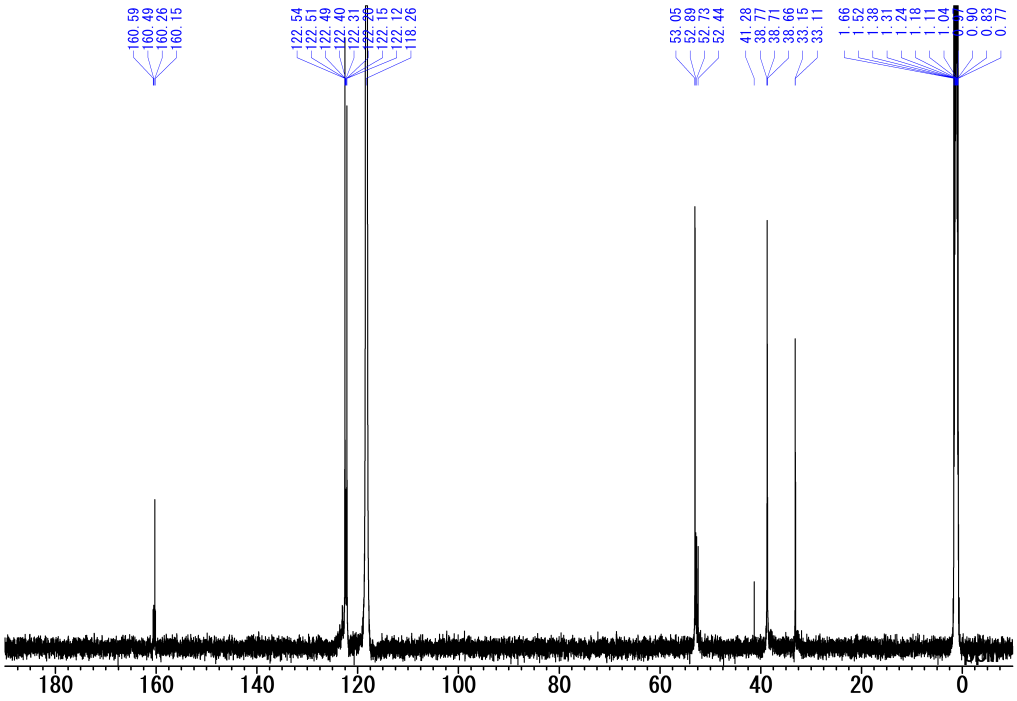

Fig. S20 ^{13}C NMR spectrum of [**Pt^{C3}$_3$**](PF$_6$)$_2$ (CD$_3$CN, 150 MHz, 293 K):

C_{3h}-isomer: δ 160.3 (2-im), 122.5 (4,5-im), 122.1 (4,5-im), 53.1 (N-CH$_2$), 38.8 (N-Me), 33.2 (-CH$_2$-).

C_s-isomer: δ 160.6 (2-im), 160.5 (2-im), 160.2 (2-im), 122.51 (4,5-im), 122.49 (4,5-im),122.39 (4,5-im), 122.31 (4,5-im), 122.26 (4,5-im), 122.2 (4,5-im), 52.9 (N-CH$_2$), 52.7 (N-CH$_2$), 52.4 (N-CH$_2$), 38.8 (N-Me), 38.7 (N-Me), 33.1 (-CH$_2$-).

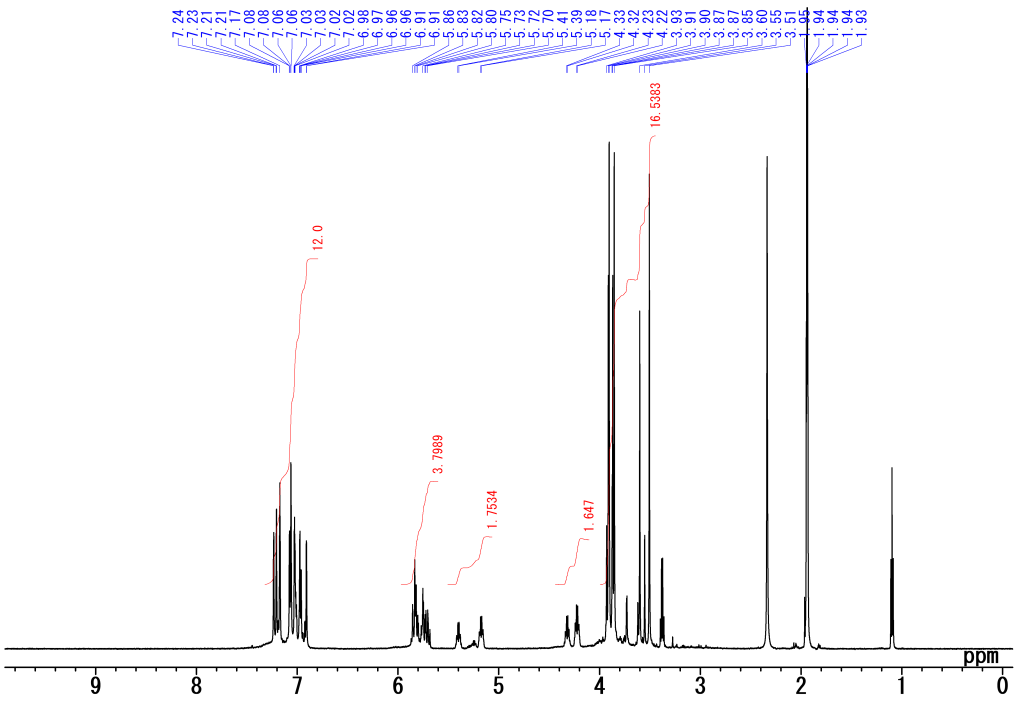

Fig. S21 ^{1}H NMR spectrum of [$\mathbf{Pt^{C1}_2Pt^{C2}}$](PF$_6$)$_2$ (CD$_3$CN, 600 MHz, 253 K):
a mixture of the isomers: δ 7.23–6.91 (m, 4,5-im), 5.87–5.68 (m, N-CH$_2$), 5.42–5.38 (m, N-CH$_2$), 5.19-5.15 (m, N-CH$_2$), 4.34–4.30 (m, N-CH$_2$), 4.24–4.20 (m, N-CH$_2$), 3.91 (s, N-Me), 3.90 (s, N-Me), 3.87 (s, N-Me), 3.85 (s, N-Me), 3.60 (s, N-Me), 3.55 (s, N-Me).

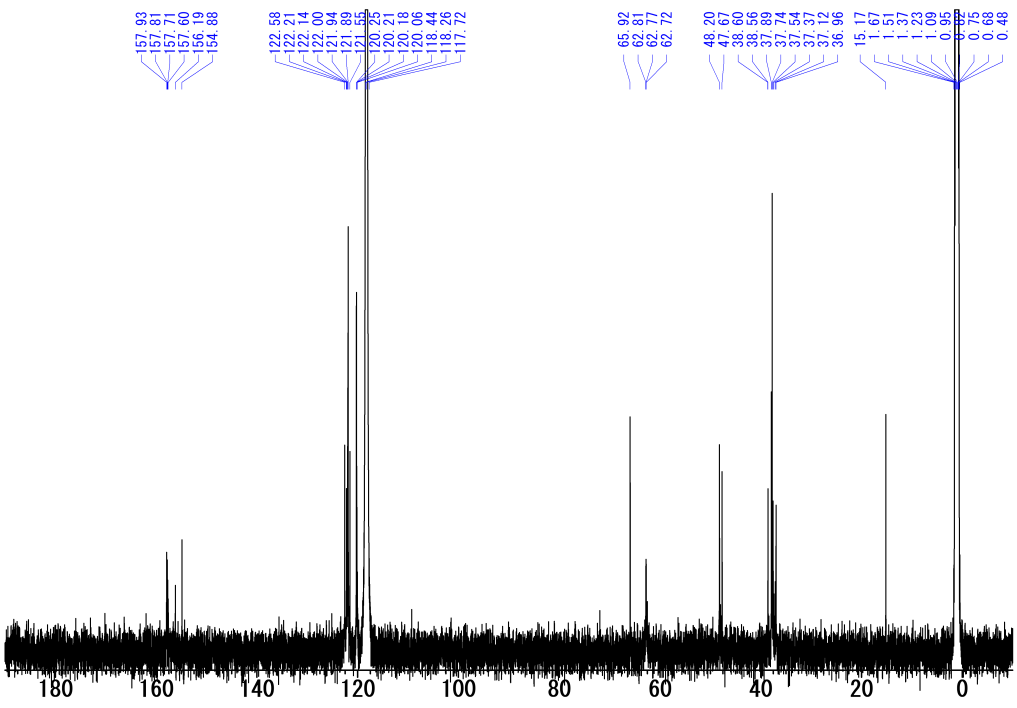

Fig. S22 ^{13}C NMR spectrum of [$\mathbf{Pt^{C1}_2Pt^{C2}}$](PF$_6$)$_2$ (CD$_3$CN, 150 MHz, 253 K):
a mixture of the isomers: δ 157.9 (2-im), 157.8 (2-im), 157.7 (2-im), 157.6 (2-im), 156.2 (2-im), 154.9 (2-im), 122.6 (4,5-im), 122.2 (4,5-im), 121.99-121.89 (4,5-im), 121.5 (4,5-im), 120.6 (4,5-im), 120.21 (4,5-im), 120.17 (4,5-im), 62.8-62.5 (N-CH$_2$-), 48.2 (N-CH$_2$-), 47.7 (N-CH$_2$-), 38.6 (N-Me), 37.9 (N-Me), 37.7 (N-Me), 37.5 (N-Me), 37.4 (N-Me), 37.1 (N-Me), 36.9 (N-Me).

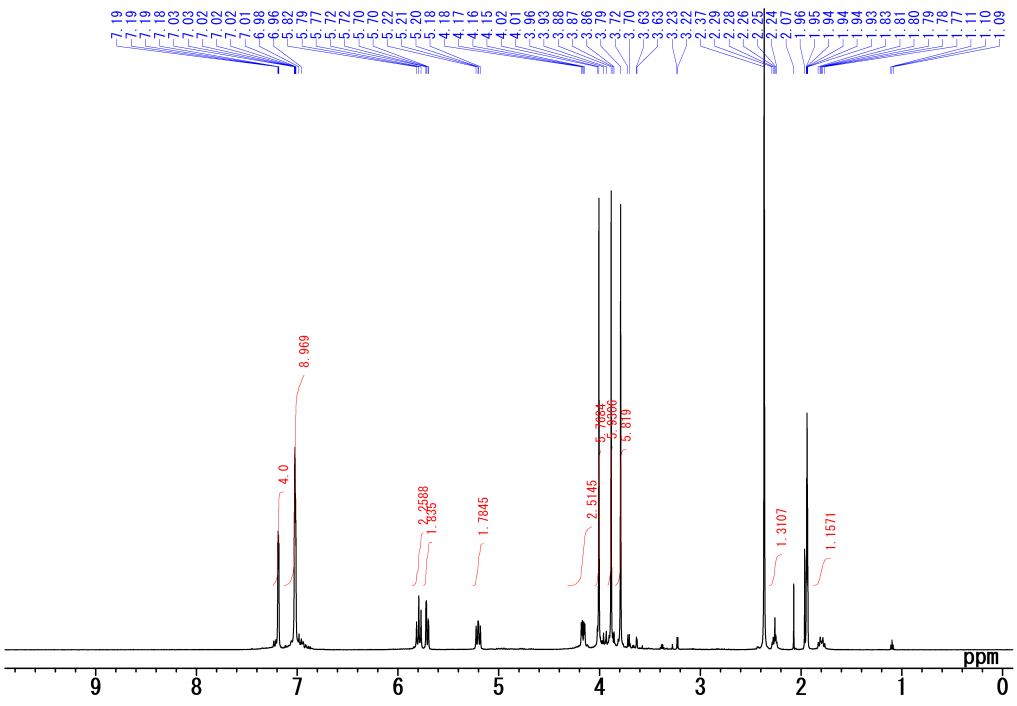

Fig. S23 ^{1}H NMR spectrum of [$\mathbf{Pt}^{\mathbf{C1}}_{2}\mathbf{Pt}^{\mathbf{C3}}$](PF$_6$)$_2$ (CD$_3$CN, 600 MHz, 253 K):
δ 7.19 (d, $^{3}J_{\text{H-H}}$ = 1.9 Hz, 2H, 4-im$^{\text{C1a}}$), 7.18 (d, $^{3}J_{\text{H-H}}$ = 1.9 Hz, 2H, 5-im$^{\text{C1a}}$), 7.03–7.01 (m, 8H, im$^{\text{C1b, C3}}$), 5.80 (d, $^{2}J_{\text{H-H}}$ = 13.2 Hz, 2H, N-CH$_2^{\text{C1}}$), 5.78 (d, $^{2}J_{\text{H-H}}$ = 13.6 Hz, 2H, N-CH$_2^{\text{C1}}$), 5.71 (d, $^{2}J_{\text{H-H}}$ = 12.9 Hz, 1H, N-CH$_2^{\text{C1}}$), 5.71 (d, $^{2}J_{\text{H-H}}$ = 12.9 Hz, 1H, N-CH$_2^{\text{C1}}$), 5.20 (dd, 2H, $^{2}J_{\text{H-H}}$ = 14.3 Hz, $^{3}J_{\text{H-H}}$ = 11.1 Hz, N-CH$_2^{\text{C3}}$), 4.16 (dd, $^{2}J_{\text{H-H}}$ = 14.2 Hz, $^{3}J_{\text{H-H}}$ = 6.1 Hz, 2H, N-CH$_2^{\text{C3}}$), 4.01 (s, 6H, N-Me$^{\text{C3}}$), 3.88 (s, 6H, N-Me$^{\text{C1a}}$), 3.79 (s, 6H, N-Me$^{\text{C1b}}$), 2.26 (ddd, $^{2}J_{\text{H-H}}$ = 16.0 Hz, $^{3}J_{\text{H-H}}$ = 6.6 Hz, $^{3}J_{\text{H-H}}$ = 6.0 Hz, 2H, N-CH$_2^{\text{C3}}$), 1H, -CH$_2$-$^{\text{C3}}$), 1.80 (ddd, $^{2}J_{\text{H-H}}$ = 16.3 Hz, $^{3}J_{\text{H-H}}$ = 10.9 Hz, $^{3}J_{\text{H-H}}$ = 10.9 Hz, 1H, -CH$_2$-$^{\text{C3}}$).

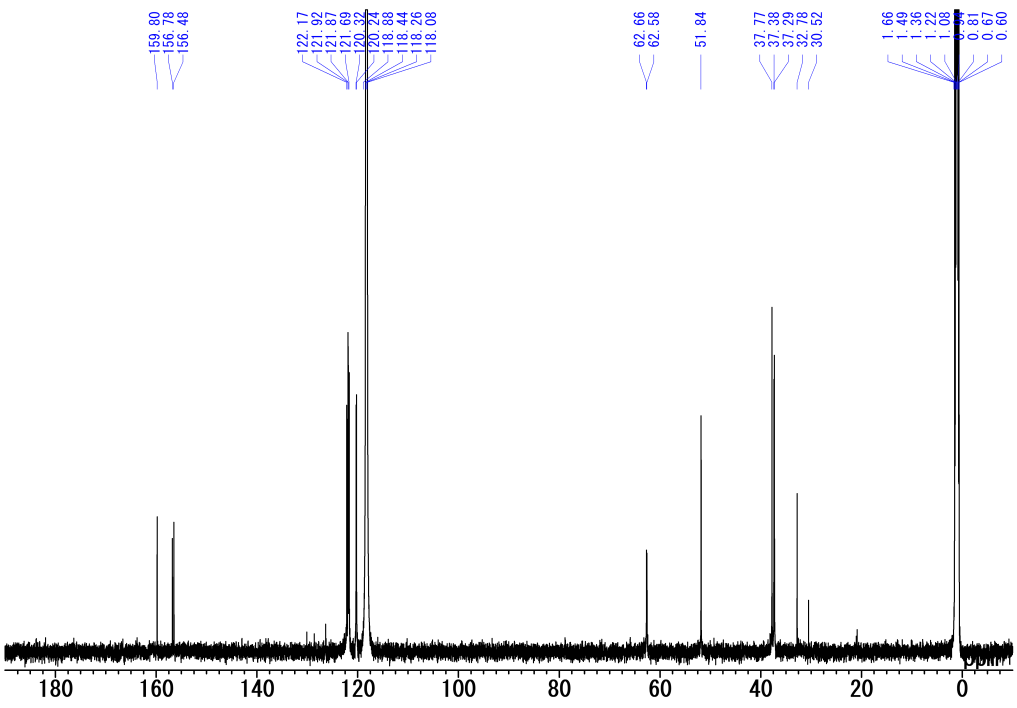

Fig. S24 ^{13}C NMR spectrum of [$\mathbf{Pt^{C1}_2Pt^{C3}}$](PF$_6$)$_2$ (CD$_3$CN, 150 MHz, 253 K):

δ 159.8 (2-im^{C3}), 156.8 (2-im^{C1a,b}), 156.5 (2-im$^{C1a.b}$), 122.2 (s, 4,5-im^{C3}), 121.92 (s, 4,5-im^{C1b,C3}),121.86 (s, 4,5-im^{C1b,C3}), 121.7 (s, 4,5-im^{C1b,C3}), 120.3 (s, 4,5-im^{C1a}), 120.2 (s, 4,5-im^{C1a}), 62.7 (s, N-CH$_2^{C1a,b}$), 62.6(s, N-CH$_2^{C1a,b}$), 51.8 (s, N-CH$_2^{C3}$), 37.8 (s, N-Me^{C3}), 37.4 (s, N-Me^{C1a}), 37.3 (s, N-Me^{C1b}), 32.8 (s, -CH$_2$-^{C3}).

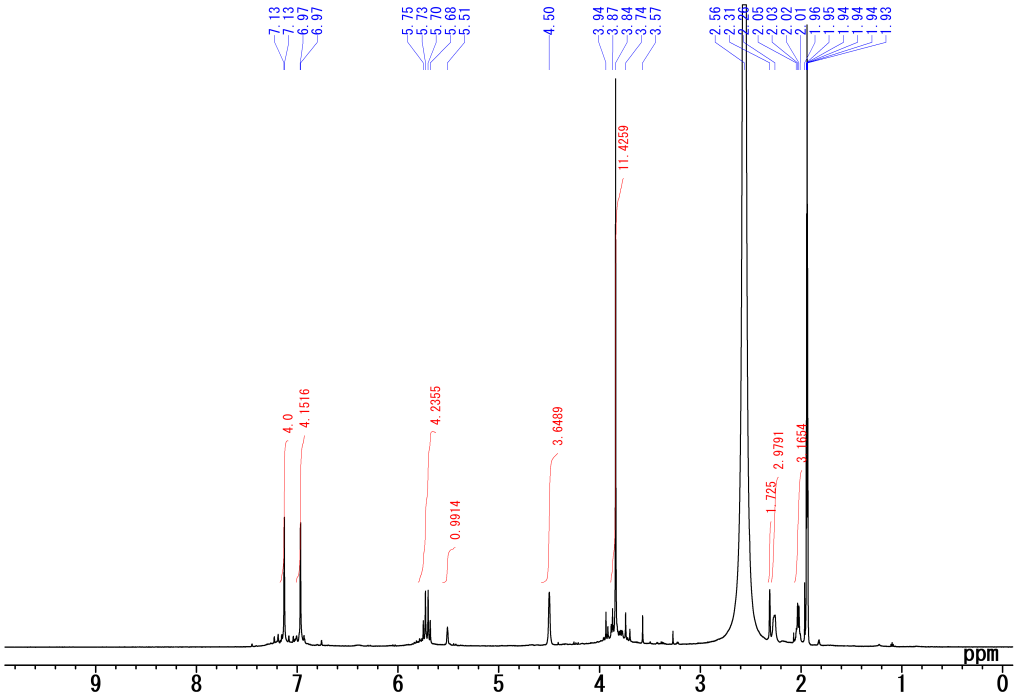

Fig. S25 ^{1}H NMR spectrum of [**Pt^{C1}$_2$Rh^{cod}**](PF$_6$) (CD$_3$CN, 600 MHz, 253 K):
δ 7.13 (d, $^{3}J_{H\text{-}H}$ = 1.9 Hz, 4H, 4-im), 6.97 (d, $^{3}J_{H\text{-}H}$ = 1.9 Hz, 4H, 5-im), 5.74 (d, $^{2}J_{H\text{-}H}$ = 12.7 Hz, 2H, N-CH$_2$), 5.69 (d, $^{2}J_{H\text{-}H}$ = 12.7 Hz, 2H, N-CH$_2$), 4.50 (br, 4H, cod-CH), 3.84 (s, 12H, N-Me), 2.26 (br, 4H, cod-CH$_2$), 2.03 (d, 4H, $^{2}J_{H\text{-}H}$ = 8.0 Hz, cod-CH$_2$).

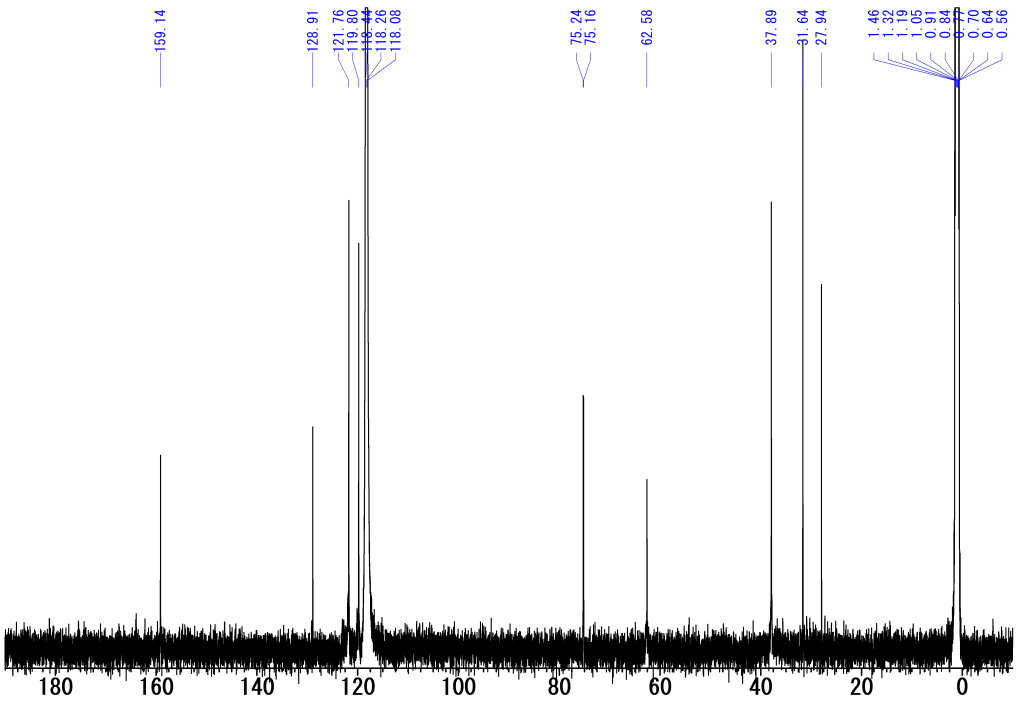

Fig. S26 ^{13}C NMR spectrum of [$\mathbf{Pt^{C1}_2Rh^{cod}}$](PF$_6$) (CD$_3$CN, 150 MHz, 253 K):
δ 159.1 (2-im), 121.8 (s, 5-im), 119.8 (s, 4-im), 75.2 (d, $^1J_{C–Rh}$ = 11.2 Hz, cod-CH), 62.6 (s, N-CH$_2$), 37.9 (s, N-Me), 31.6 (s, cod-CH$_2$).

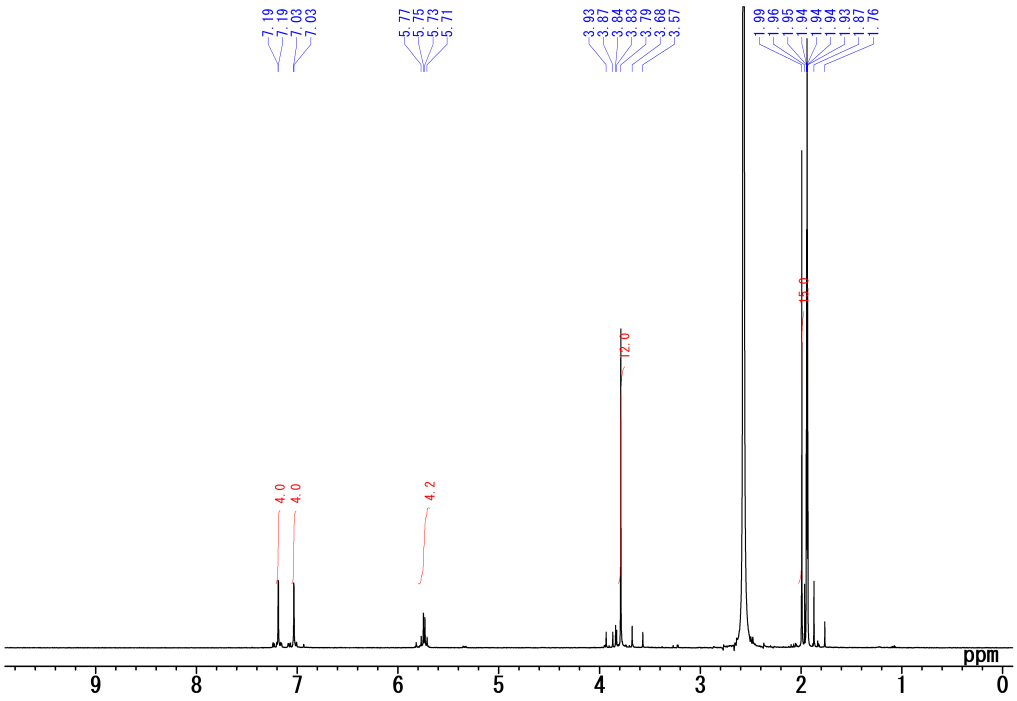

Fig. S27 ^{1}H NMR spectrum of [$\mathbf{Pt^{Cl}_2Rh^{Cp^*}}$](PF$_6$)$_2$ (CD$_3$CN, 600 MHz, 253 K): δ 7.19 (d, $^{3}J_{\text{H-H}}$ = 1.9 Hz, 4H, 4-im), 7.03 (d, $^{3}J_{\text{H-H}}$ = 1.9 Hz, 4H, 5-im), 5.76 (d, $^{2}J_{\text{H-H}}$ = 12.9 Hz, 2H, N-CH$_2$), 5.72 (d, $^{2}J_{\text{H-H}}$ = 12.9 Hz, 2H, N-CH$_2$), 3.79 (s, 12H, N-Me), 1.99 (s, 15H, Cp*-Me).

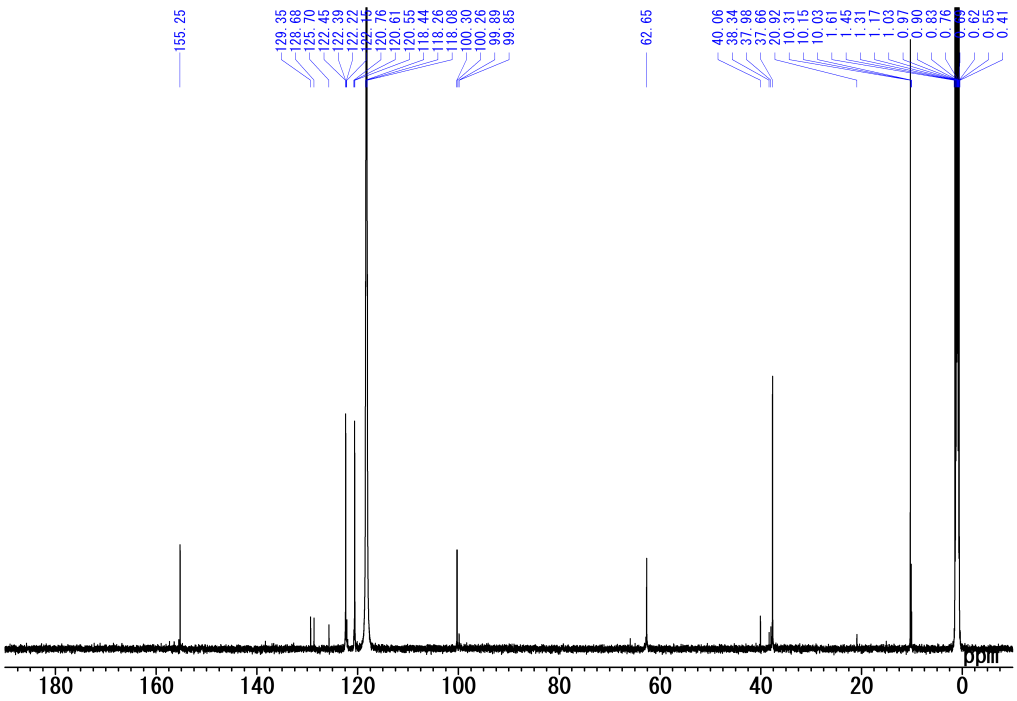

Fig. S28 ^{13}C NMR spectrum of [$\mathbf{Pt^{C1}_2Rh^{Cp*}}$](PF$_6$)$_2$ (CD$_3$CN, 150 MHz, 253 K):
δ 155.3 (2-im), 122.4 (s, 5-im), 120.6 (s, 4-im), 100.3 (d, $^1J_{C–Rh}$ = 7.2 Hz Cp*-ring), 62.6 (s, N-CH$_2$), 37.7 (s, N-Me), 10.3 (s, Cp*-Me).

7. Electrospray ionisation mass spectrometry

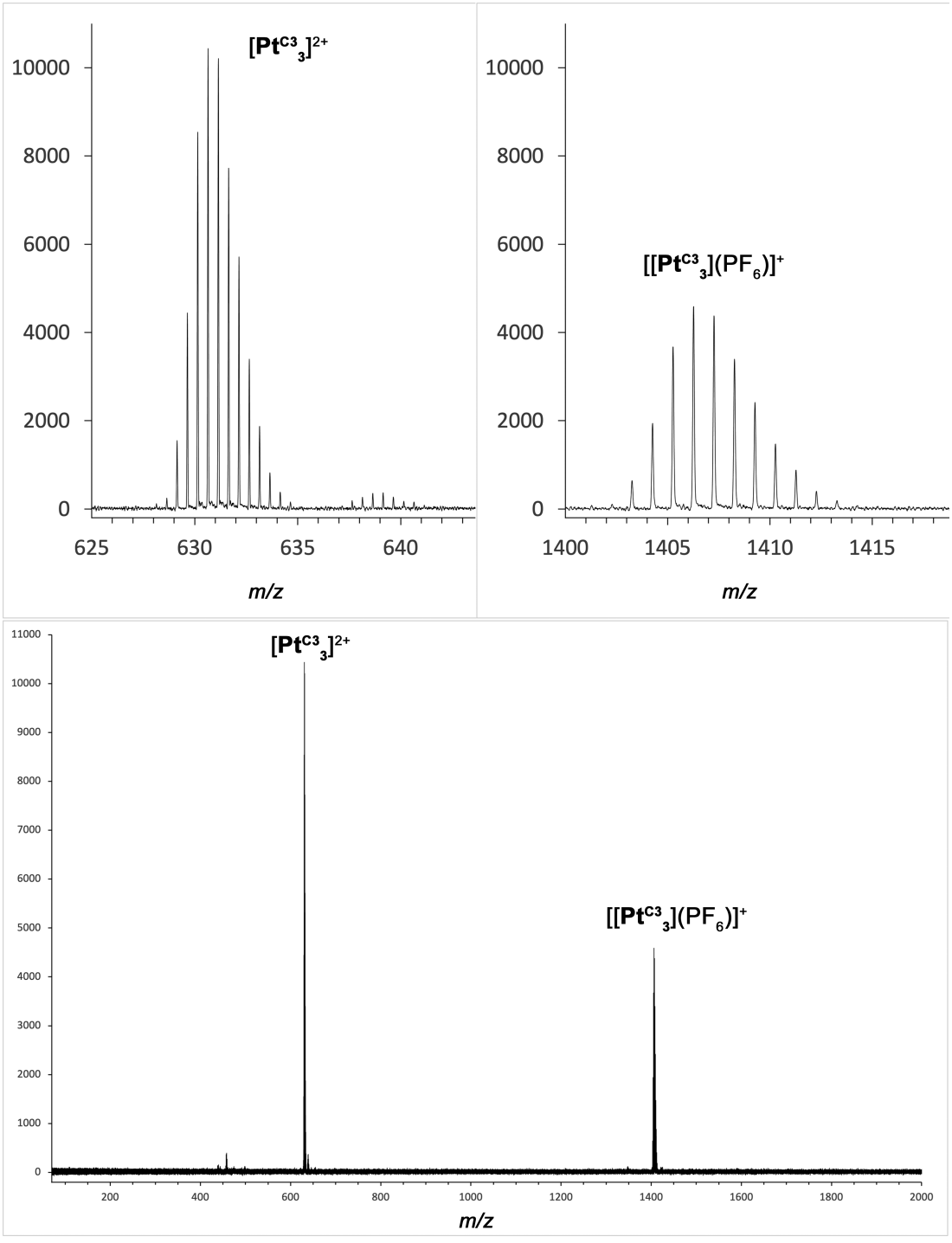

Fig. S29 ESI-mass spectrum of $[\mathbf{Pt}^{\mathbf{C3}}{}_3](PF_6)_2$ in CH_3CN.

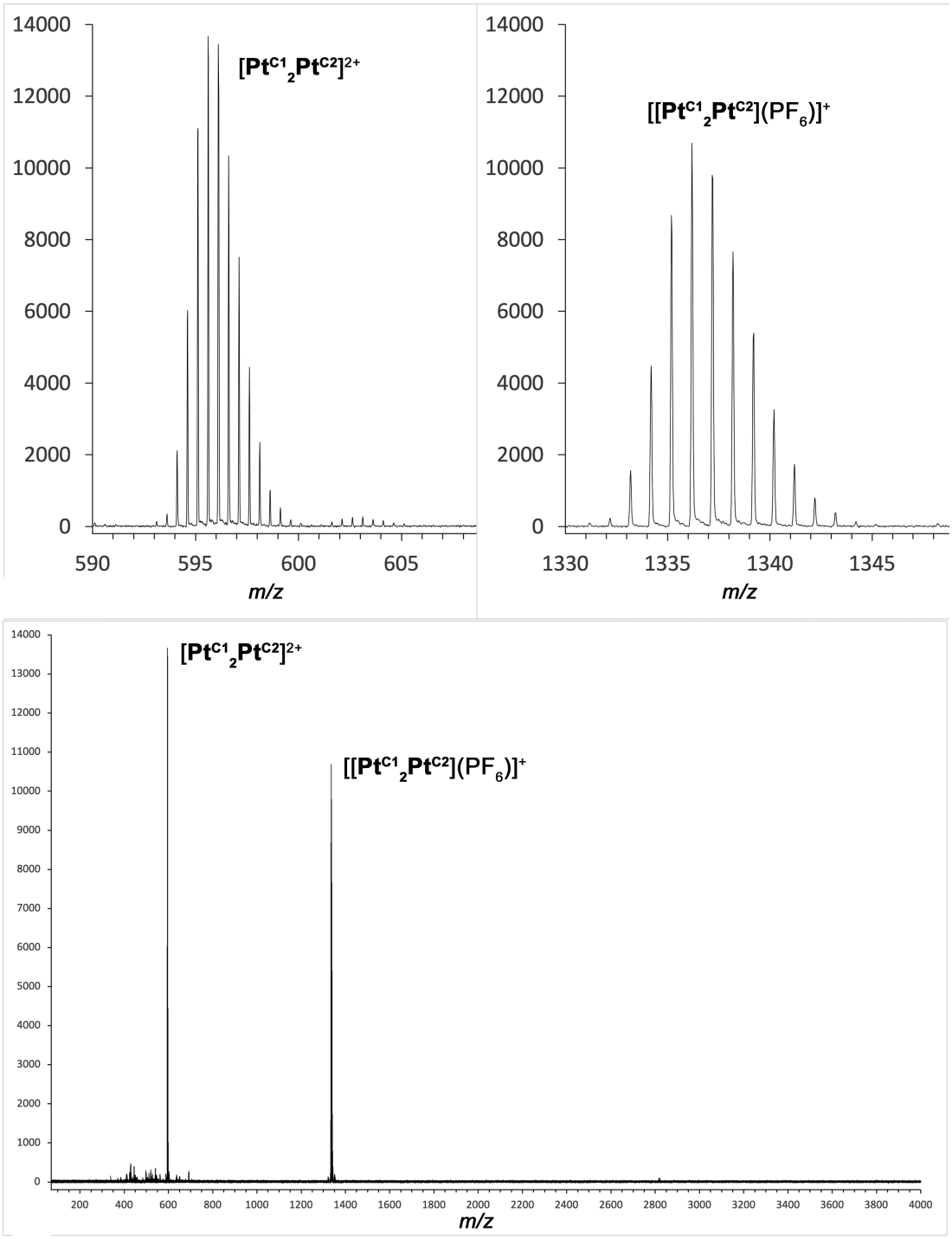

Fig. S30 ESI-mass spectrum of $[\mathbf{Pt}^{\mathbf{C1}}{}_2\mathbf{Pt}^{\mathbf{C2}}](PF_6)_2$ in CH_3CN.

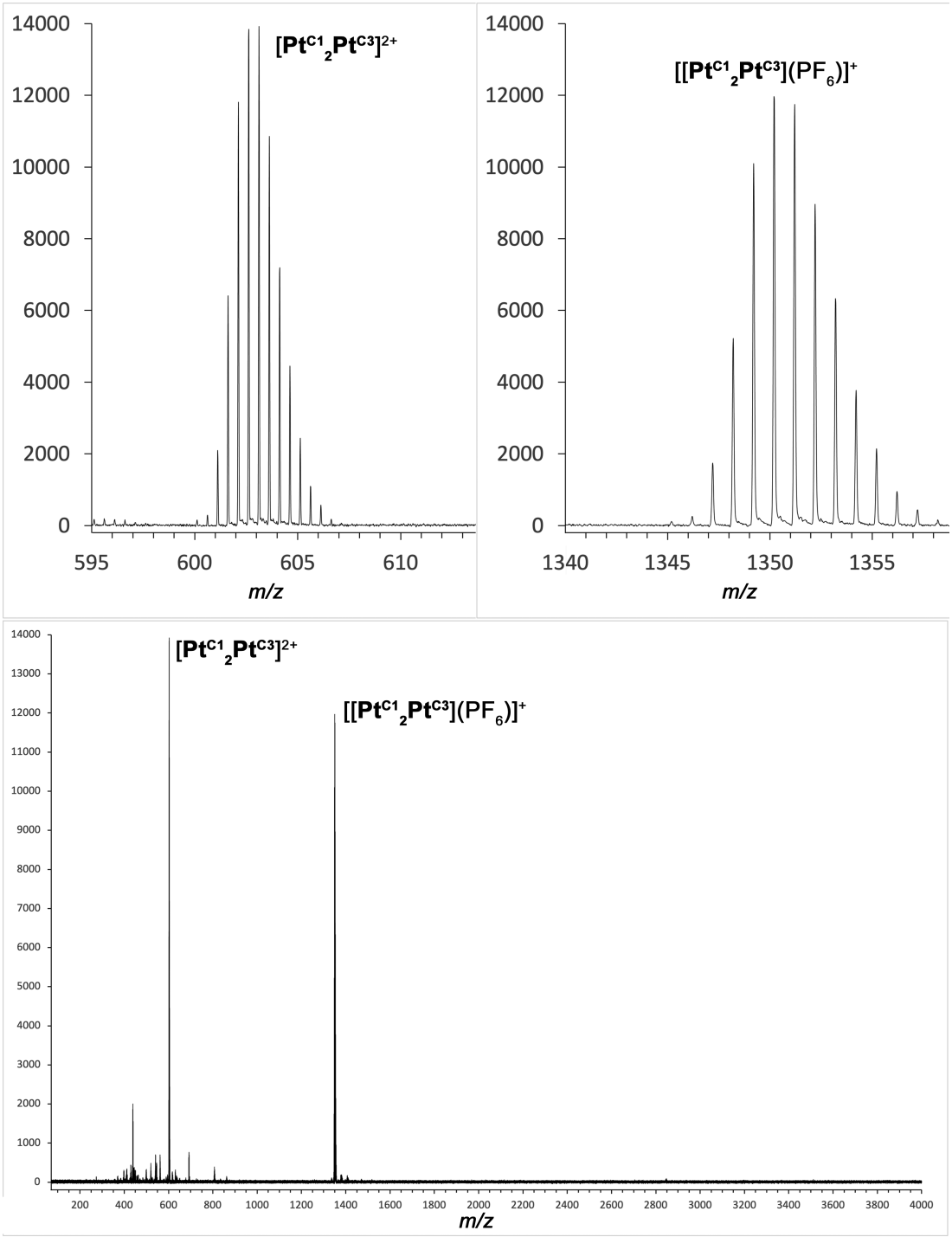

Fig. S31 ESI-mass spectrum of $[\mathbf{Pt}^{\mathbf{C1}}{}_2\mathbf{Pt}^{\mathbf{C3}}](PF_6)_2$ in CH_3CN.

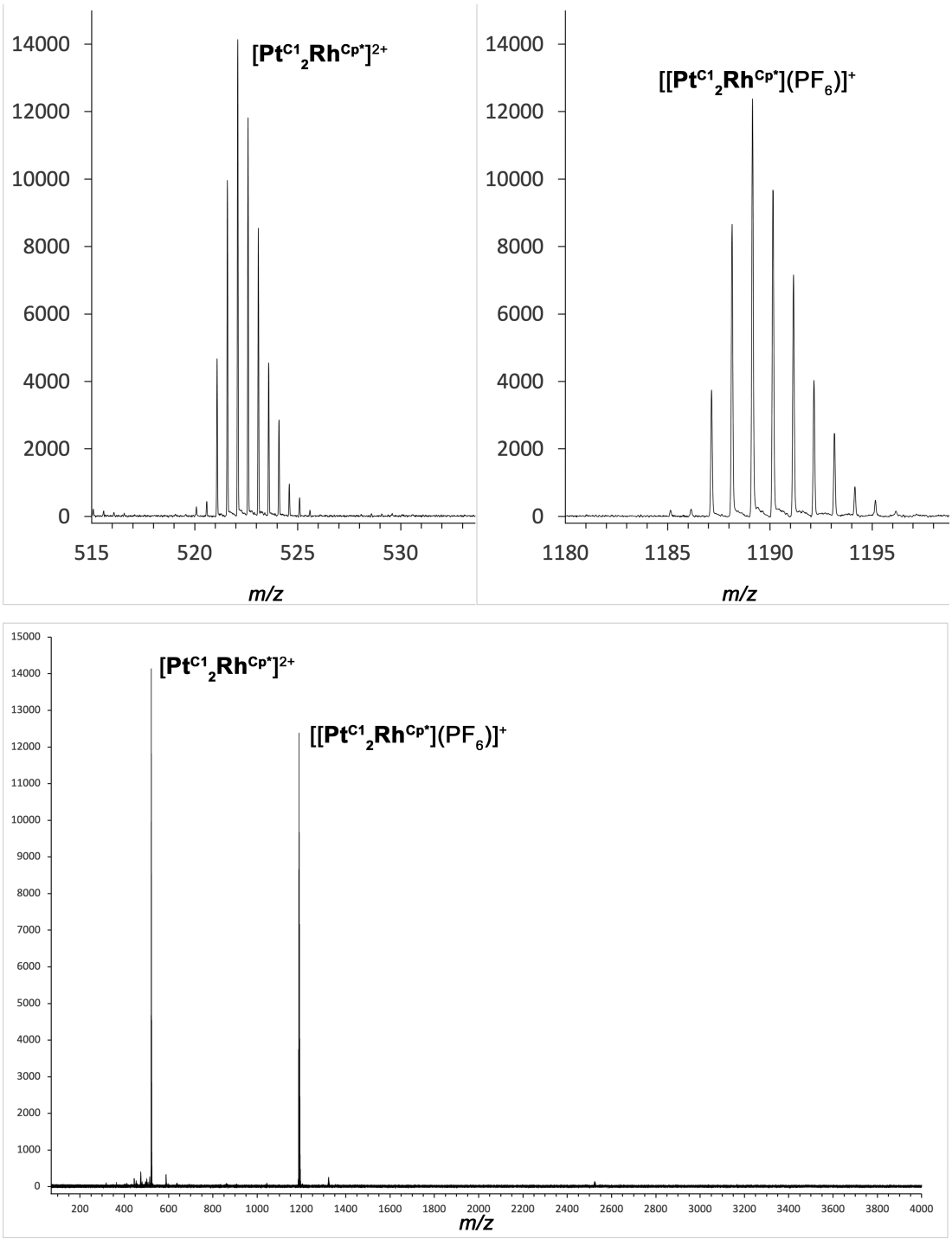

Fig. S32 ESI-mass spectrum of $[\mathbf{Pt}^{\mathbf{C1}}{}_2\mathbf{Rh}^{\mathbf{Cp^*}}](PF_6)_2$ in CH_3CN.

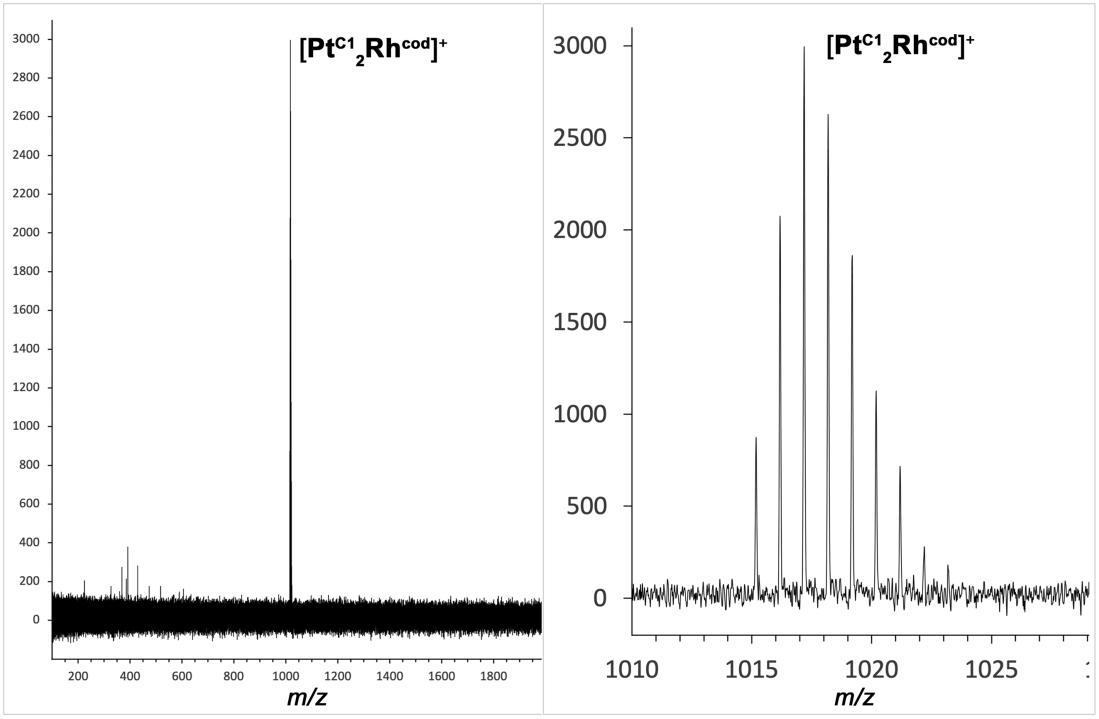

Fig. S33 ESI-mass spectrum of [$\mathbf{Pt^{C1}_2Rh^{cod}}$]($PF_6$) in CH_3CN.

8. Reference

1. A. L. Spek, *Acta Cryst.*, 2015, **C71**, 9–18.